

NON-UNIQUENESS OF THE MODELED MAGNETIZATION VECTORS USED IN
DETERMINING PALEOPOLES ON MARS

by
Saurav Biswas
B.Sc., Calcutta University, 2000
M.Sc., University of Pune, 2002

A Thesis
Submitted in Partial Fulfillment of the Requirements for
The Master of Science Degree

Department of Geology
In the Graduate School
Southern Illinois University Carbondale
December 2005

THESIS APPROVAL

NON-UNIQUENESS OF THE MODELED MAGNETIZATION VECTORS USED IN
DETERMINING PALEOPOLES ON MARS

By

Saurav Biswas

A Thesis Submitted in Partial

Fulfillment of the Requirements for

Master of Science Degree

Approved by:

Dr. Dhananjay Ravat, Chair

Dr. Eric Ferre

Dr. Scott Ishman

Graduate School
Southern Illinois University Carbondale
August 2005

AN ABSTRACT OF THE THESIS OF

Saurav Biswas, for the Master of Science Degree in Geology, presented on August 5, 2005, at Southern Illinois University Carbondale.

TITLE: Non-uniqueness of the Modeled Magnetization Vectors Used in Determining Paleopoles on Mars

MAJOR PROFESSOR: Dhananjay Ravat

This study investigates the non-uniqueness of current magnetization models derived from magnetic anomalies on Mars observed by the Mars Global Surveyor spacecraft. The alternative multiple source configurations developed in this study demonstrate that these sources can explain the anomalies designated as M10 and M3 on Mars equally well as the models derived by Arkani-Hamed (2001, 2002), Arkani-Hamed and Boutin (2003, 2004), Hood and Zakharian (2001) and Richmond and Hood (2003) based on large elliptical or circular prismatic sources, and Frawley and Taylor (2004) based on Helbig method. The results of this study suggest that many of the large isolated magnetic anomalies observed on Mars could be produced by the coalescence effect of differently magnetized smaller sources. The resulting scatter in paleopole locations computed from the alternative multiple source configurations covers nearly 40% of the surface of Mars and, thus, the utility of these paleopole locations in deciphering the ancient tectonics is questioned. Furthermore, the paleopoles computed from the large elliptical or circular prismatic sources require the following special assumptions:

- Only small lateral lithospheric movement, if any, between the sources of identified anomaly since acquisition of their magnetization.
- Correct estimation of the source geometry – shape and size.

In a comparative scenario on Earth, the 2D model of the near-surface anomaly over northeast American and neighboring Atlantic ocean on Earth and the 3D models of the satellite altitude anomaly over the same region demonstrated that magnetic models based on the Amplitude of Analytic Signal (AAS) field were similar to the near-surface magnetic anomaly patterns which closely reflect the geology, whereas, the model deciphered from the Z-component magnetic field alone was significantly different. This suggests on Mars the magnetic model based on the AAS field is likely to yield better source characteristics than modeling of Z-component magnetic field.

ACKNOWLEDGEMENTS

First of all I would like to thank my advisor, Dr. Dhananjay Ravat for providing me with this wonderful opportunity to pursue research on Mars. His ability to solve most of my computer or research related problems by working across different time zones in the world is gratefully acknowledged.

I am grateful to my parents and sister for being supportive of my decisions which have brought me here. I must say, Christopher, your friendship is very valuable. You made the ‘cultural shock’ of being in a new country seem not so shocking. Rich, I must acknowledge your incredible ability to deal with computers when they misbehave. I could not have accomplished my thesis without your help. I am grateful to all my friends at Carbondale for making these last three years memorable. I must thanks Sonja and Sharon for always being available to help me. I must thank Dr. Roger Phillips, Washington University, St. Louis for very fruitful discussion on this research. I would like to thank Dr. P.T. Taylor of NASA, GSFC for giving me the permission to use his figure. I would also like to thank Dr. Hugh Miller, Memorial University of Newfoundland for providing useful reference on the geology of Newfoundland.

TABLE OF CONTENTS

ABSTRACT.....	i
ACKNOWLEDGEMENTS	iii
LIST OF TABLES	v
LIST OF FIGURES	vi
CHAPTER 1	1
CHAPTER 2	9
CHAPTER 3	28
CHAPTER 4	43
CHAPTER 5	46
REFERENCES	48
VITA.....	52

LIST OF TABLES

TABLE 2.1	11
TABLE 2.2	17
TABLE 3.1	35
TABLE 3.2	38

LIST OF FIGURES

FIGURE 1.1	2
FIGURE 1.2	3
FIGURE 1.3	6
FIGURE 2.1	10
FIGURE 2.2	14
FIGURE 2.3	15
FIGURE 2.4	16
FIGURE 2.5	19
FIGURE 2.6	21
FIGURE 2.7	22
FIGURE 2.8	24
FIGURE 2.9	25
FIGURE 2.10	26
FIGURE 3.1	29
FIGURE 3.2	30
FIGURE 3.3	32
FIGURE 3.4	34
FIGURE 3.5	36
FIGURE 3.6	39
FIGURE 3.7	40

CHAPTER 1

INTRODUCTION

The magnetic anomalies observed by the Mars Global Surveyor (MGS) spacecraft (Figure 1.1) are attributed to strong remanent magnetization in the crust (Acuna et al., 1999; Connerney et al., 1999). The magnetic data collected by the spacecraft are classified in different phases: the aero-braking (AB) and science-phasing orbits (SPO) with altitude ranging between 85 to 170 km and the mapping orbit with average altitude of about 400 km (Acuna et al., 2001). It is generally believed that Mars had a global core-generated magnetic field early in its geologic history, which ceased to exist around 3.9 billion years ago (Acuna et al., 1999); although, Schubert et al. (2000) have argued that the Martian dynamo turned on after 4 billion years ago and turned off at an unknown time since then. Based on small amplitude anomalies from the electron reflection magnetometer data occurring within the large impact craters previously considered demagnetized, Lillis et al. (2005) have recently suggested that a second period of dynamo activity may have occurred approximately 300 million years after the cessation of early dynamo.

The anomalies at altitudes greater than 100 km have very large amplitudes (± 1500 nT) (Connerney et al., 1999) over the southern highland region and appear as broad, continuous, high and low bands over Terra Cimmeria and Terra Sirenum (Figure 1.2) (Purucker et al., 2000). Near the northern latitudes the magnetic anomalies are almost isolated and appear as small patches of magnetic highs and lows over Planum Boreum and Vastitas Borealis (Figure 1.2) (Hood and Zakharian, 2001) and are also present over

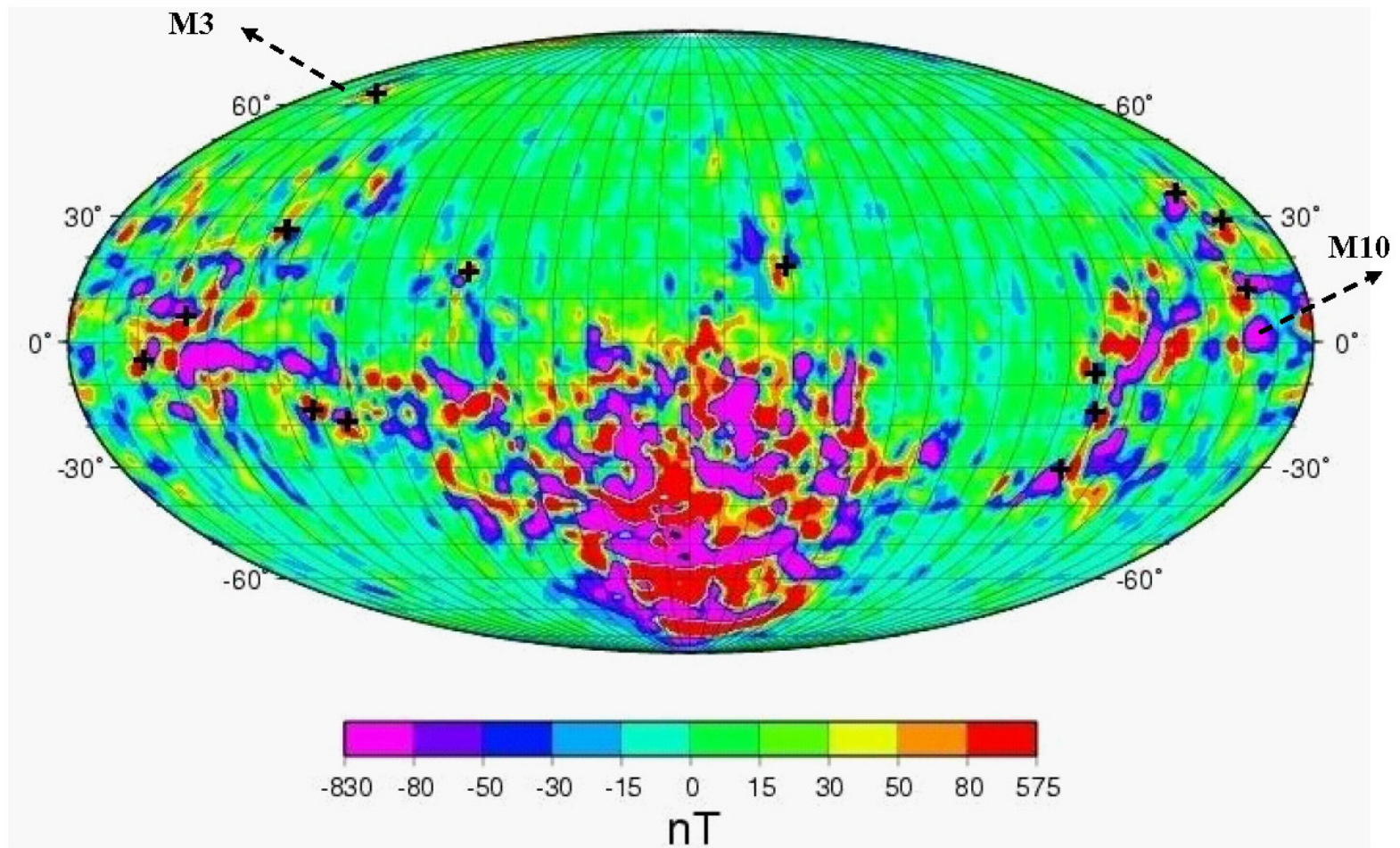


Figure 1.1. Z-component magnetic anomaly map of Mars (centered at 180° E, Mollweide projection) observed by MGS satellite compiled using the equivalent source method (Purucker et al., 2000). The + symbol denotes the near horizontally magnetized anomalies.

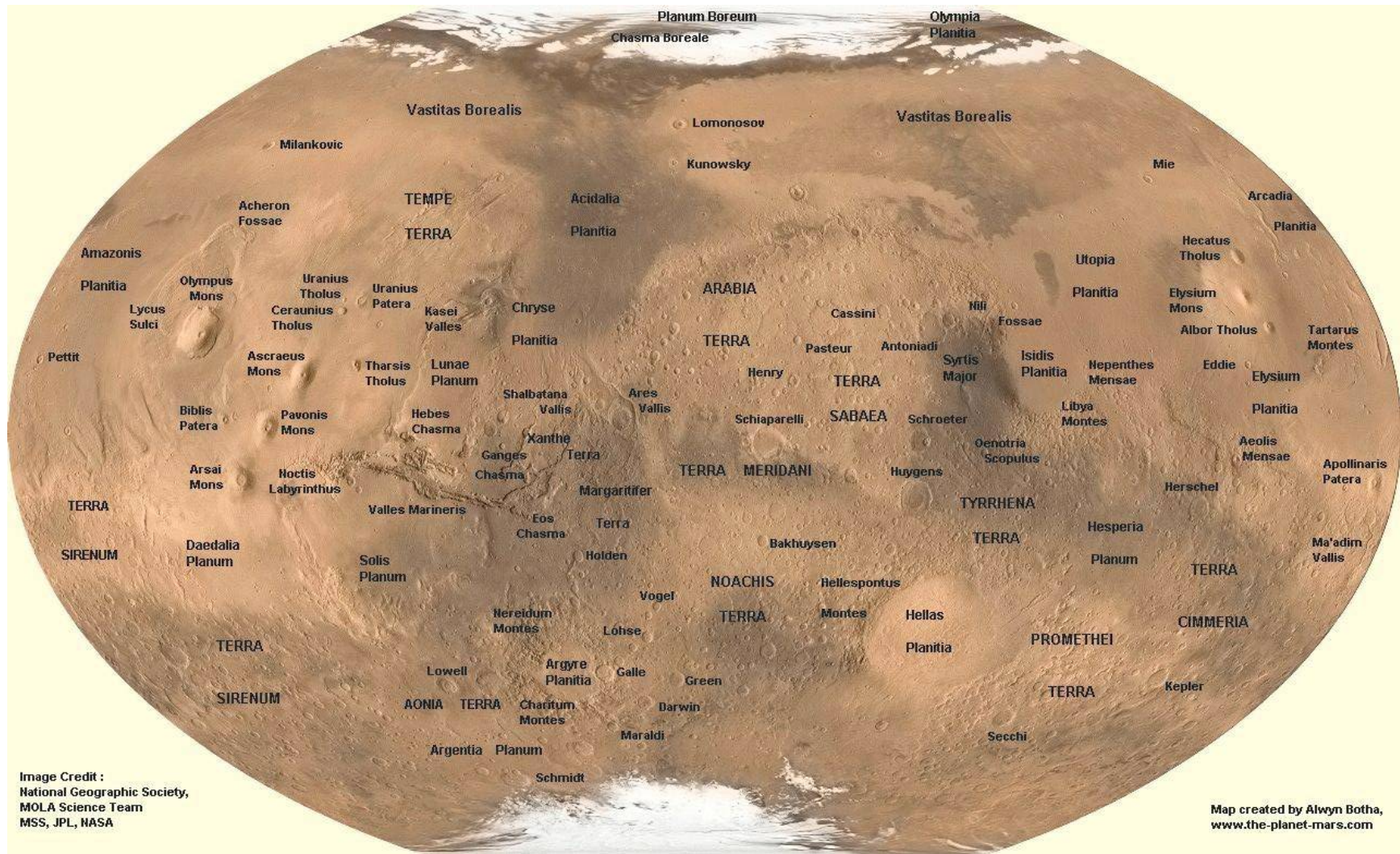


Figure 1.2 A map (centered at 0°, Winkel-Tripel projection) showing the physiographic regions of Mars. The projection and longitude range of this figure is different than figure 1.1. Longitude 180° E – 180° W.

equatorial and sub-equatorial regions (Arkani-Hamed, 2001, 2002; Richmond and Hood, 2003) of Mars. Connerney et al. (2001), Arkani-Hamed (2001, 2002), Hood and Zakharian (2001), Phillips (2003) and Ravat and Miller (2004) have modeled some of these anomalies using different approaches. Arkani-Hamed (2001) and Arkani-Hamed and Boutin (2003, 2004) have used uniformly magnetized elliptical prismatic sources to model 16 semi-isolated anomalies. Hood and Zakharian (2001) and Richmond and Hood (2003) have used uniformly magnetized circular bodies to model anomalies near the northern latitudes of Mars. Phillips (2003) has applied the Helbig method (Phillips, 2003) to deduce the magnetization directions and strengths of the remanent crustal magnetic field. Ravat and Miller (2004) have modeled simultaneously the Z-component and Amplitude of Analytic Signal (AAS) field in the southern highlands of Mars to model the magnetization vectors. Most researchers have used the modeled inclination angle (I) and declination angle (D) of the magnetization vectors to compute the paleopole of Mars. Arkani-Hamed (2001) inferred a paleopole position with a circle of confidence of 30° radius centered at 230°E, 25°N. Hood and Zakharian (2001) derived a paleopole position centered at 135°W, 50°N. Phillips (2003) calculated his paleopole positions within 50 degrees of 195°E, 50°N. Frawley and Taylor (2004) using Helbig method showed that some of the same anomalies modeled by the earlier workers could be modeled with different magnetization vectors. There is significant dispersion in the paleopole positions computed by different authors and they have suggested scenarios of pole reversals, secular variation and true polar wander on Mars as explanations (Arkani-Hamed, 2001; Hood and Zakharian, 2001; Phillips, 2003; Arkani-Hamed and Boutin, 2004; Frawley and Taylor, 2004). Langlais et al. (2004) suggest that the technique used in deriving the

paleopole positions in the above cases (specially Arkani-Hamed, 2001 and Hood and Zakharian, 2001) is reliable if one assumes that the source bodies are homogeneously magnetized.

Modeling magnetic anomalies on Mars (from satellite altitudes) is subject to non-unique solutions inherent to potential fields. Green's theorem of the equivalent layer shows that a potential can be caused by an infinite variety of sources (e.g., Blakely, 1995). This suggests that, in addition to the source configurations of existing models, there could be other plausible source configurations producing similar magnetic anomalies but having different magnetization vectors. In addition, the observation of magnetic field at satellite altitude is subject to coalescence of anomalies (e.g., Ravat and Miller, 2004; Biswas and Ravat, 2005), which is not accounted for in the interpretation by previous authors. Coalescence of the observed anomalies makes it difficult to infer the precise geologic nature of the sources and their true magnetization directions. The coalescence effect can be described as attenuation and merging together of neighboring short-wavelength anomalies into regionally larger anomalies at higher altitudes. Figure 1.2 shows the profiles of magnetic field (F) and gradient of the field ($\text{Grad } F$) across three sets of dikes at 125 and 10 km elevations. At 125 km elevation, the magnetic field profile shows a single broad high whereas at 10 km elevation three distinct signatures are clearly observed. This shows that at higher altitudes the short-wavelength pattern of the field attenuates and merges together into a single long-wavelength feature. The profile of the field gradient at 125 km can still show three distinct highs, although it suppresses the finer short-wavelength features present in the profile at 10 km. This figure, therefore, also illustrates that computing the gradient of the field might provide us with a better tool in

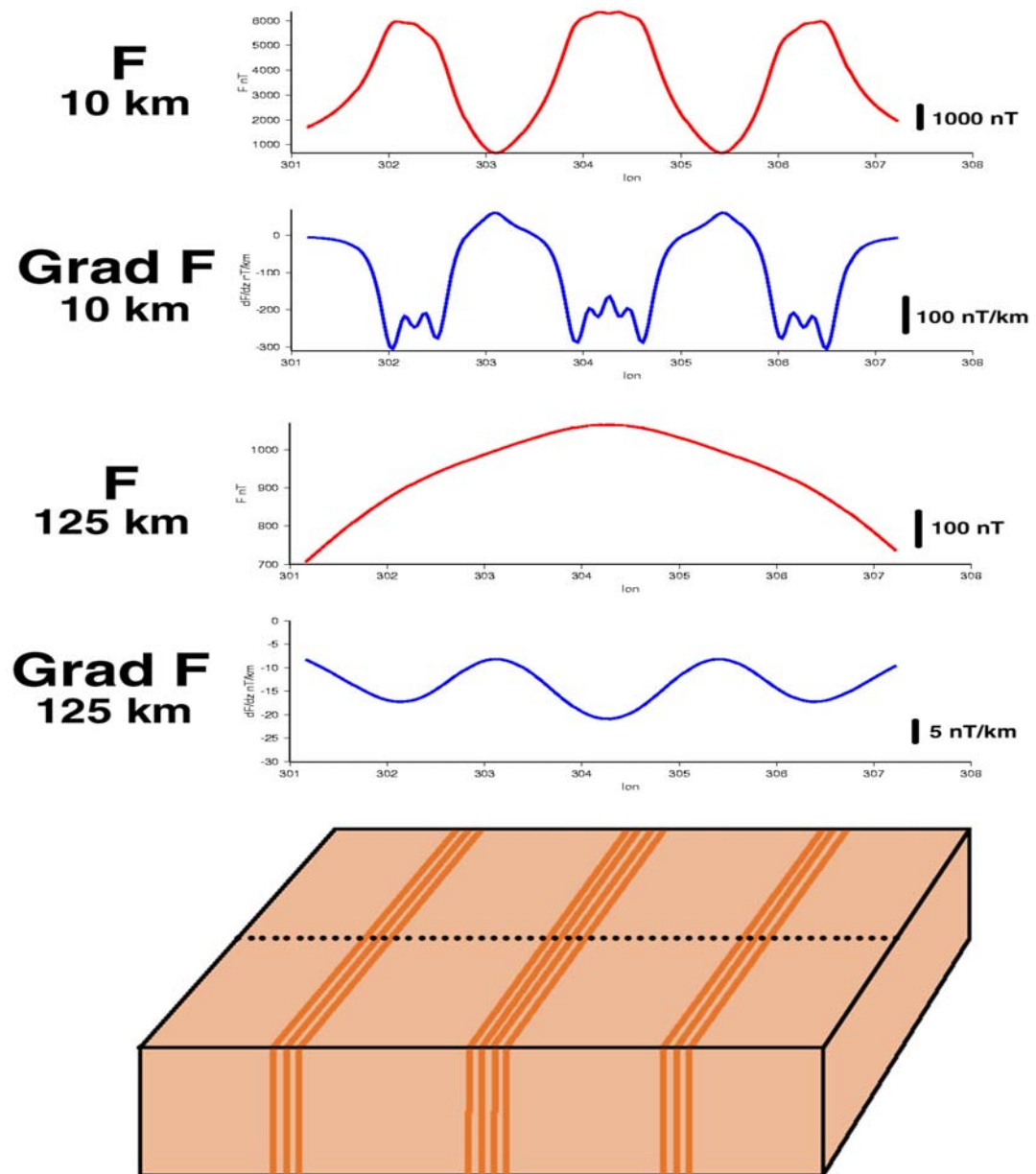


Figure 1.3. A figure showing profiles of magnetic anomaly data at 125 km and 10 km elevations to illustrate the coalescence effect. (courtesy P.T. Taylor, personal communication, 2005)

delineating outline of different sources from satellite altitude data. I apply this principle with the help of the technique known as the amplitude of Analytic Signal (AAS) for designing the source outlines for my models of the magnetic anomalies.

Another facet of the anomaly coalescence is demonstrated by Carporzen et al. (2005) and Dunlop (2005). Their study over the Vredefort meteorite crater shows that impact acts to increase the magnetization in the shocked rocks; however, the magnetization direction varies significantly over short distances indicating that the magnetization is not controlled primarily by the planetary field but the intense fields generated during the shock. This random appearing strong magnetization effectively cancels out by interference at higher altitude, leading to small anomaly values observed in the aeromagnetic surveys. Thus when observed from high altitude, one may not be able to see any significant increase in the magnetic intensity signature over the impact craters. They suggest this phenomenon as an explanation for significantly lower magnetic field intensities observed on Mars by the MGS satellite over the gigantic impact craters Hellas and Argyre than over surrounding regions. In contrast, the present thinking is that the Hellas and Argyre basins were formed by impacts which occurred after the Martian dynamo had shut down in the past. However, the results of Lillis et al. (2005), related to observation of small intensity magnetic fields within the large craters, could be reinterpreted within the context of the above shock impact model of Carporzen et al. (2005).

It may not be feasible to recover the detailed picture of magnetization from satellite altitude data because some of the short-wavelength anomalies have been completely attenuated. Therefore, one needs to investigate whether alternative source geometries for

the anomalies would lead to sufficiently similar I and D angles as the sources modeled by the earlier researchers, or completely different magnetization angles would be possible.

This study investigates the non-uniqueness in the magnetic anomaly models from alternative source configurations and the coalescence effect in the satellite altitude data using forward modeling of some of the Mars and Earth based magnetic anomalies.

CHAPTER 2

DEMONSTRATION OF NON-UNIQUENESS USING ALTERNATIVE SOURCE CONFIGURATIONS

First, a simple model is used to demonstrate the non-uniqueness in the source configurations of magnetic anomaly models with the following example. I have designed 3 E-W oriented prismatic sources which are $1^\circ \times 3^\circ$ in their dimensions (Figure 2.1a). The thickness of the sources is 10 km. A computer program, MARSPHERE, designed to forward model magnetic anomaly components from remanently magnetized prismatic sources on a spherical planet, based on a program designed for Earth by von Frese et al. (1981) was used to produce the Z-component magnetic field. The northernmost source is oppositely magnetized (Strength = 5 A/m, $I = -45^\circ$, $D = 30^\circ$) compared to the southern two sources (Strength = 5 A/m, $I = 45^\circ$, $D = 30^\circ$). The oblique inclination (45°) of the remanent sources leads to a dipolar Z-component anomaly. Figures 2.1b to 2.1f show alternative single source models for the anomaly produced by the three source configuration of Figure 2.1a. The angle of declination for the single source is 13° , not 30° as in the original sources. Furthermore, there is a wide range of magnetization vectors ranging from $I = 10^\circ - 70^\circ$ which could reproduce the anomaly with a bulk source of comparable size (Figure 2.1b – 2.1f) as shown in Table 1.1. Table 1 also shows the results of comparison in the form of correlation coefficient between the anomalies of three prismatic sources and each of the bulk sources. According to correlation coefficients, the source with $I = 10^\circ$ (Figure 2.1b) best approximates the anomaly of three prisms; however, visually any of these anomalies could be considered reasonable forward models matching the anomaly of Figure 2.1a. The inclinations in these

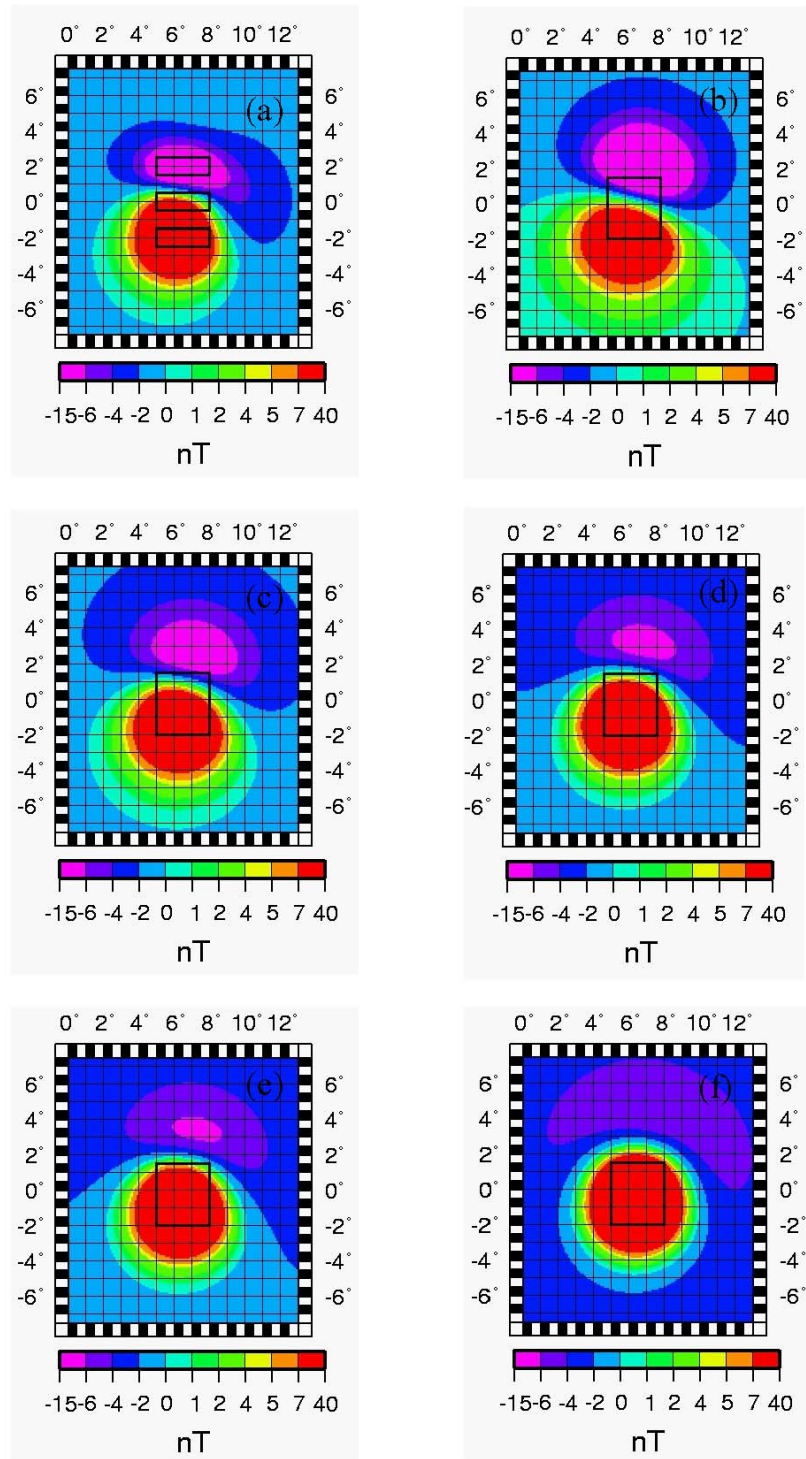


Figure 2.1. The demonstration of ambiguity in modeling the magnetization vector. Dipolar magnetic field produced by 3 EW oriented prismatic sources (a). A similar magnetic field is produced by a bulk source having different magnetization vectors (b-f).

Table 2.1. Magnetic parameters of the prismatic sources and bulk body sources.

Fig. No.	Inclination (°)	Declination (°)	Depth (km)	Magnetization (A/m)	Correlation Coefficient (No. of points = 19781)
1a	North – -45 Central – 45 Southern – 45	30	0-40	5	-
1b	10	13	0-40	5	0.93
1c	30	13	0-40	5	0.92
1d	45	13	0-40	5	0.83
1e	50	13	0-40	5	0.79
1f	70	13	0-40	5	0.61

examples vary from 10° to 70° and, using formulas in Butler (1992) would imply the angular distances to paleopoles ranging from 76° to 35° , respectively.

The converse of the above situation is also possible. The anomaly produced by a bulk single source could be matched by the anomaly of multiple segmented/fragmented sources. This suggests that the large elliptical (Arkani-Hamed, 2001) or circular (Hood and Zakharian, 2001) sources used in modeling the isolated magnetic anomalies on Mars could similarly be modeled using alternative source configurations with different magnetization vectors. Arkani-Hamed (2001) and Arkani-Hamed and Boutin (2004) have used large elliptical sources to model 16 different isolated magnetic anomalies on Mars. To show the non-uniqueness in their models, I have chosen two different anomalies, designated as M10 and M3 by Arkani-Hamed (2001) from the Z-component altitude-normalized equivalent source magnetic anomaly map of Mars at 150 km (similar to Purucker et al., 2000) and also demonstrate the possibility of alternative source configurations and coalescence effect. The Z-component anomaly pattern of M10 has only a single lobe and is consistent with a vertically magnetized single source.

Our approach in demonstrating the ambiguity from alternative source models of isolated anomalies is as follows. First, we create a forward model of the approximate source simulating the observed Z-component field from the steepest gradients of the Amplitude of Analytic Signal (AAS) field (similar to Ravat and Miller, 2004). Ravat and Miller (2004) showed that for forward modeling it is convenient to begin with the outline of the steepest gradient of the AAS field. Then I use different classes of alternate source configurations (e.g., segmented linear sources of narrow width, fragmented sources) and magnetizations that would lead to the observed Z-component anomaly. Finally, I

compute paleopoles from the derived magnetization vectors to show that they can be dispersed for the segmented and fragmented models. The segmented models represent but few of the many geologic scenarios and, therefore, only a few of many different sets of resulting paleopoles.

The AAS field of Z-component anomaly M10 (contours in Figure 2.2a) implies that if a single source were responsible for the anomaly it would be magnetized with orientation nearly vertically upward (source outline and its modeled field is shown in Figure 2.2b). In the forward modeling, source geometry, angles of inclination and declination, and magnetization strength are varied till the modeled anomaly reasonably matches the observed anomaly. The orientation of the magnetization vector for my model of the elliptical source is $I = -85^\circ$ and $D = 212^\circ$. The thickness of the source is 20 km. Yet, the same anomaly could be approximately reproduced with a narrow linear 40 km thick source (Figure 2.2c). Furthermore, many different sources with different magnetizations can also lead to the same anomaly as a result of anomaly coalescence (its constructive and destructive interference) with altitude. To demonstrate this, I used segmented narrow linear sources (Figure 2.2d), some having completely different magnetization directions (Table 1.2). These magnetizations would result in four significantly different paleopole locations (Table 1.2). Figure 2.3 shows that the profiles of observed and computed Z-component fields for the segmented model of M10 are in agreement with each other. To further demonstrate the coalescence effect explicitly, I computed and mapped the magnetic anomaly produced by the model representing anomaly M10 at different elevations varying from 10 km to 120 km (Figure 2.4). The anomaly at 10 km (Figure 2.4a) shows a number of positive and negative lobes associated

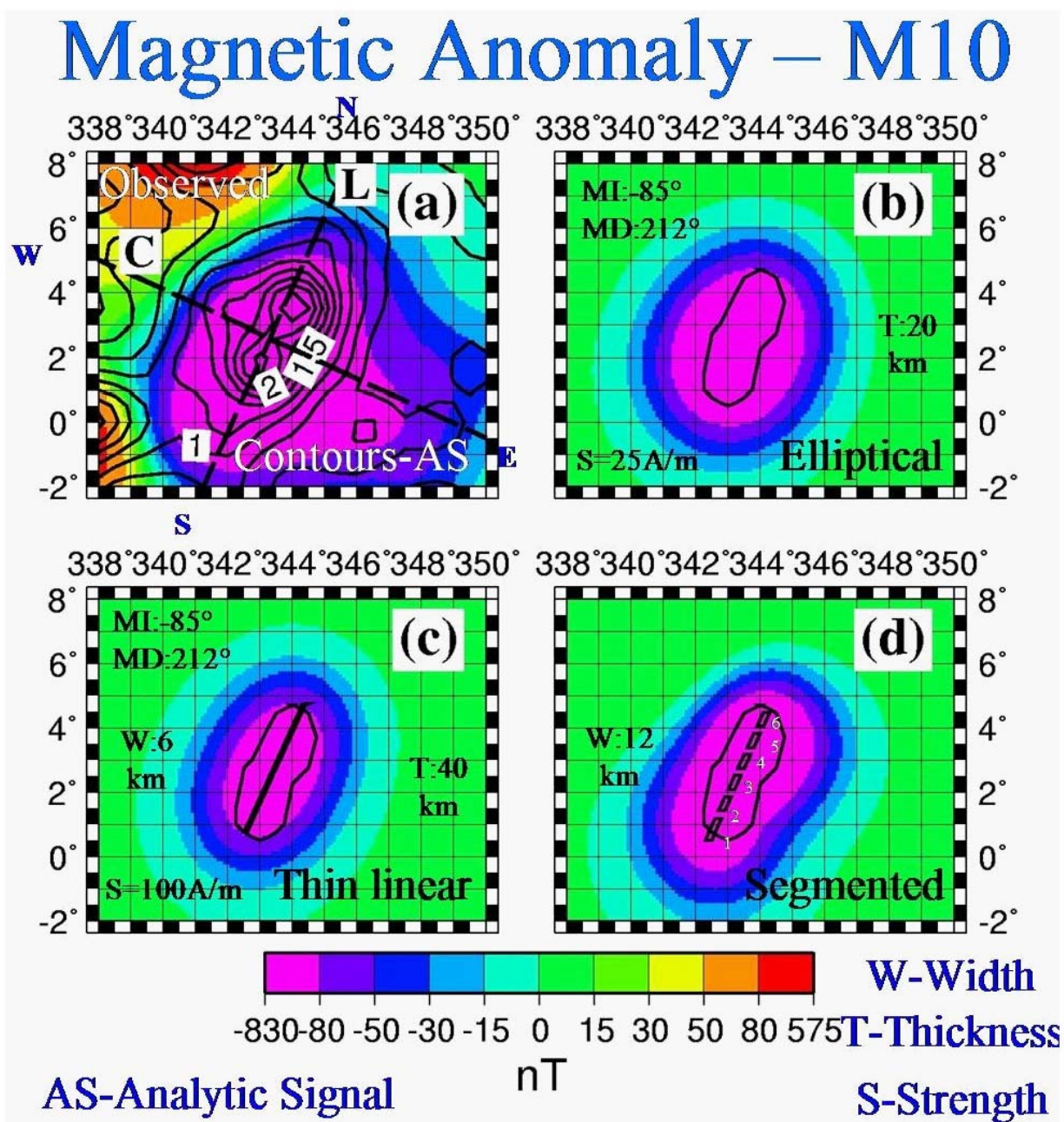


Figure 2.2. Observed magnetic anomaly M10 and alternative source models. C - Cross profile, L - Long profile, MI - Modeled Inclination, MD - Modeled Declination.

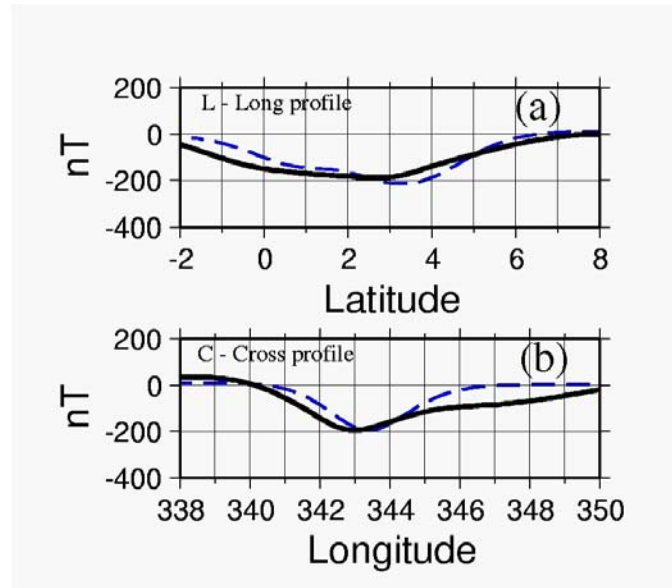


Figure 2.3. Fit of observed (continuous) and computed (dashed) Z-component fields for segmented model of M10.

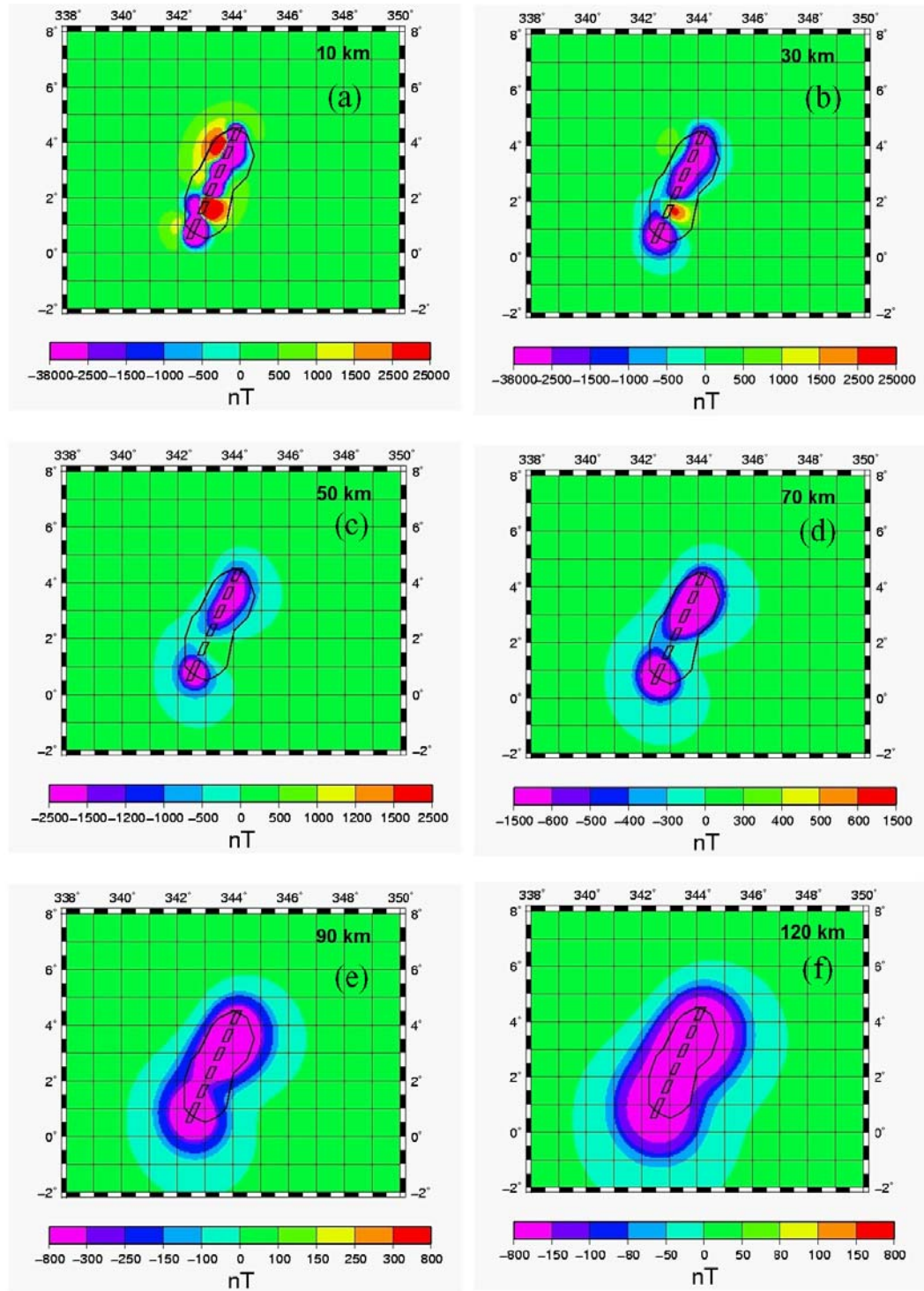


Figure 2.4. The magnetic anomaly of the segmented model of M10 computed at different elevations demonstrating the coalescence effect.

Table 2.2. Directions of modeled magnetization vectors and the respective paleopole locations for different segments in the models illustrated in Figures 2.2d and 2.5c.

Segment		Magnetization Vector			Paleopole positions	
		Inclination	Declination	Strength (A/m)	Latitude	Longitude
M10	1	-70°	130°	300	23°	313°
	2	030°	270°		0°	269°
	3	-70°	130°		24°	314°
	4	-85°	212°		11°	349°
	5	-45°	130°		37°	285°
	6	-85°	212°		13°	349°
M3	A6-7, B4-7, C2-5, D1-3, E1	-1°	335°	25	21°	231°
	A4-5, B2-3	-10°	320°	15	13°	245°
	A1-3, B1	20°	150°	12	10°	232°
	D4-5, E2-3	-10°	345°	15	19°	220°
	E4-5, F2-3	30°	160°	8	8°	223°
	M3_2	-15°	170°	14.5	35°	219°

with the different magnetization directions (Table 1.2) of different segments of the multiple source model of M10. With increase in elevation the positive portions of the anomaly attenuates and completely disappears above 50 km. The neighboring negative portions of the anomaly merge into one another with increase in elevation and become much larger in size, ultimately taking a large nearly elliptical shape at 120 km. With increase in elevation the detailed features of an anomaly are lost and with it we lose any information associated with those details (means they are present, but not visible). At 10 km, the anomaly clearly suggests multiple segmented sources; however, at 120 km one could be tempted to infer that the anomaly is produced by a large single elliptical source. This implies that interpretation of similar anomalies observed on Mars and modeled as large single sources might not be correct.

The Z-component anomaly pattern of M3 is made up of a low to the north, an elongated high in the center with two lobes and a low to the south. This complex anomaly pattern could not be reproduced with a single source. It is consistent with at least two different polygonal sources horizontally magnetized in two different directions (Figure 2.5a). The source geometry of the two polygons (Figure 2.5b) is derived beginning from the steepest gradient of the AAS field as before. The polygons are 20 km thick. The orientation of the magnetization vector for polygon M3_1 (in Figure 2.5b) is $I = -1^\circ$ and $D = 335^\circ$ and for polygon M3_2 is $I = -15^\circ$ and $D = 170^\circ$. It should be clearly noted that the low-high-low pattern of the magnetic anomaly M3 is distinctively different from the anomaly pattern modeled by Arkani-Hamed (2001) and Hood and Zakharian (2001). They had modeled only the northern two anomaly lobes (representing the northern of the two sources modeled here) produced by a single source and ignored the contribution to

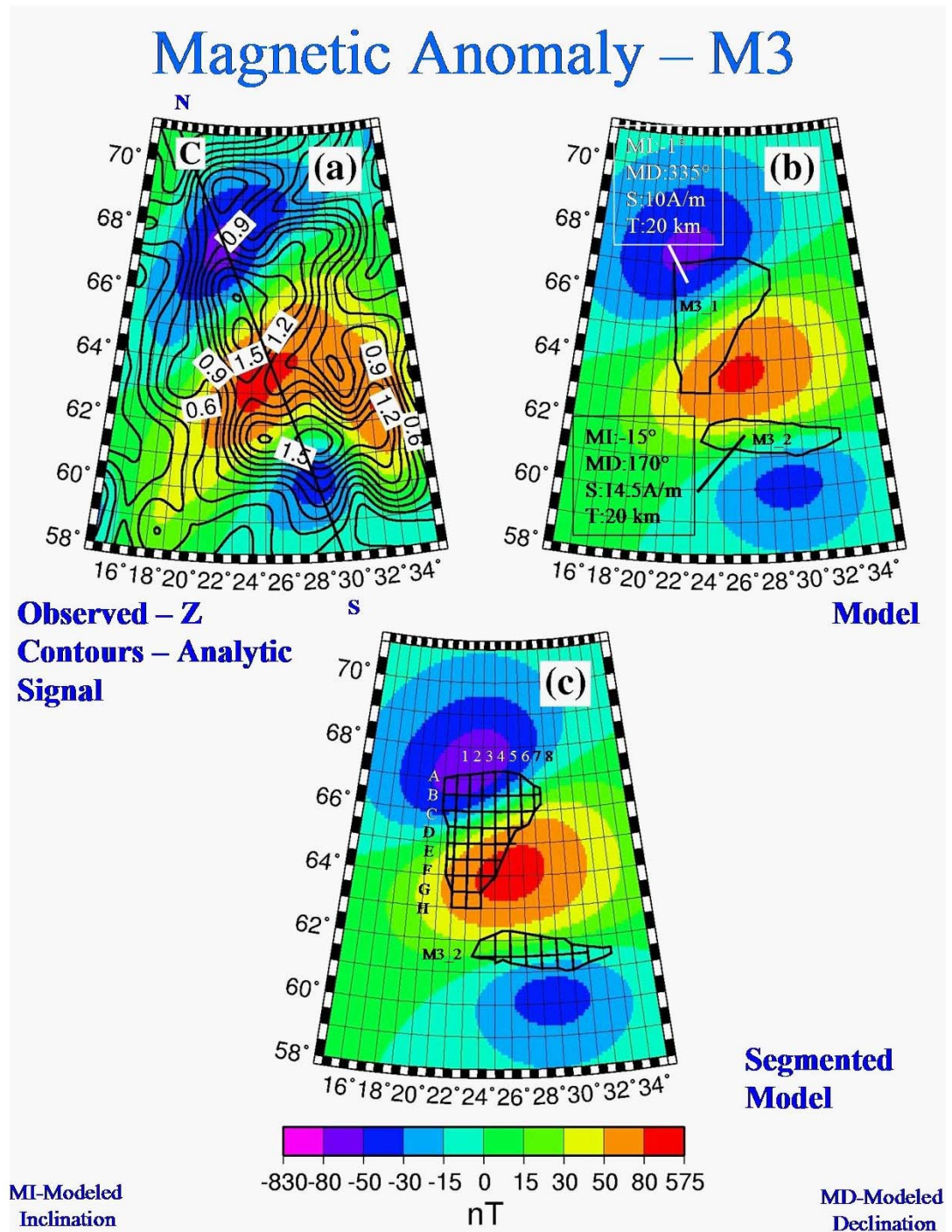


Figure 2.5. Observed near horizontally polarized magnetic anomaly – M3 and alternative source models. C – Cross profile, S – Strength, T – Thickness.

the central positive anomaly lobe from the southern source. This has resulted in different magnetization directions among the results of our studies.

The alternative source configuration with fragmented polygons (Figure 2.5c) is designed to demonstrate the ambiguity in source geometry and problem due to the coalescence effect. It matches the observed anomaly equally well. The different sets of polygons have different magnetization vectors, producing different paleopoles as shown in Table 1.2. Figure 2.6 shows that the profiles of observed and computed Z-component fields for the model of M3 agree with each other.

In addition to the Z-component, I have also computed the X and Y components of my 2 polygon model of the anomaly M3 (Figure 2.7, b-d). The observed X and Y components are plotted in the Figure 2.7 (a-b) for comparison. The features of the anomaly in my model and the observed data broadly agree with each other, suggesting that my models based on Z-component data lead to reasonable X and Y components.

I have also compared the Z-component anomaly of my model of M3 at 400 km elevation (Figure 2.7, f) with the clean Z-component data at 400 km compiled by Connerney et al. (2001) (Figure 2.7, e). The location of the main features of the anomaly in the modeled data and the observed field corresponds with each other.

It has just been illustrated that alternative source configurations like segmented linear sources for M10 or polygons for M3, with varying magnetization vectors could equally well explain the magnetic anomalies observed on Mars at 150 km altitude. If it is assumed that the anomalies observed at 150 – 400 km altitude are caused by a few large source configurations, then the location of the paleopoles computed from them depends on the magnetization directions inferred from the shape of these anomalies.

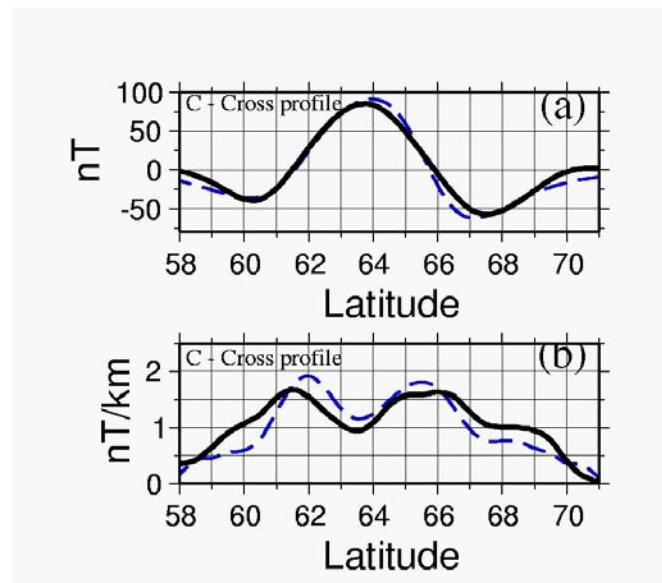


Figure 2.6. Fit of observed (continuous) and computed (dashed) Z-component (a) and Analytic Signal (b) fields of fragmented model of M3.

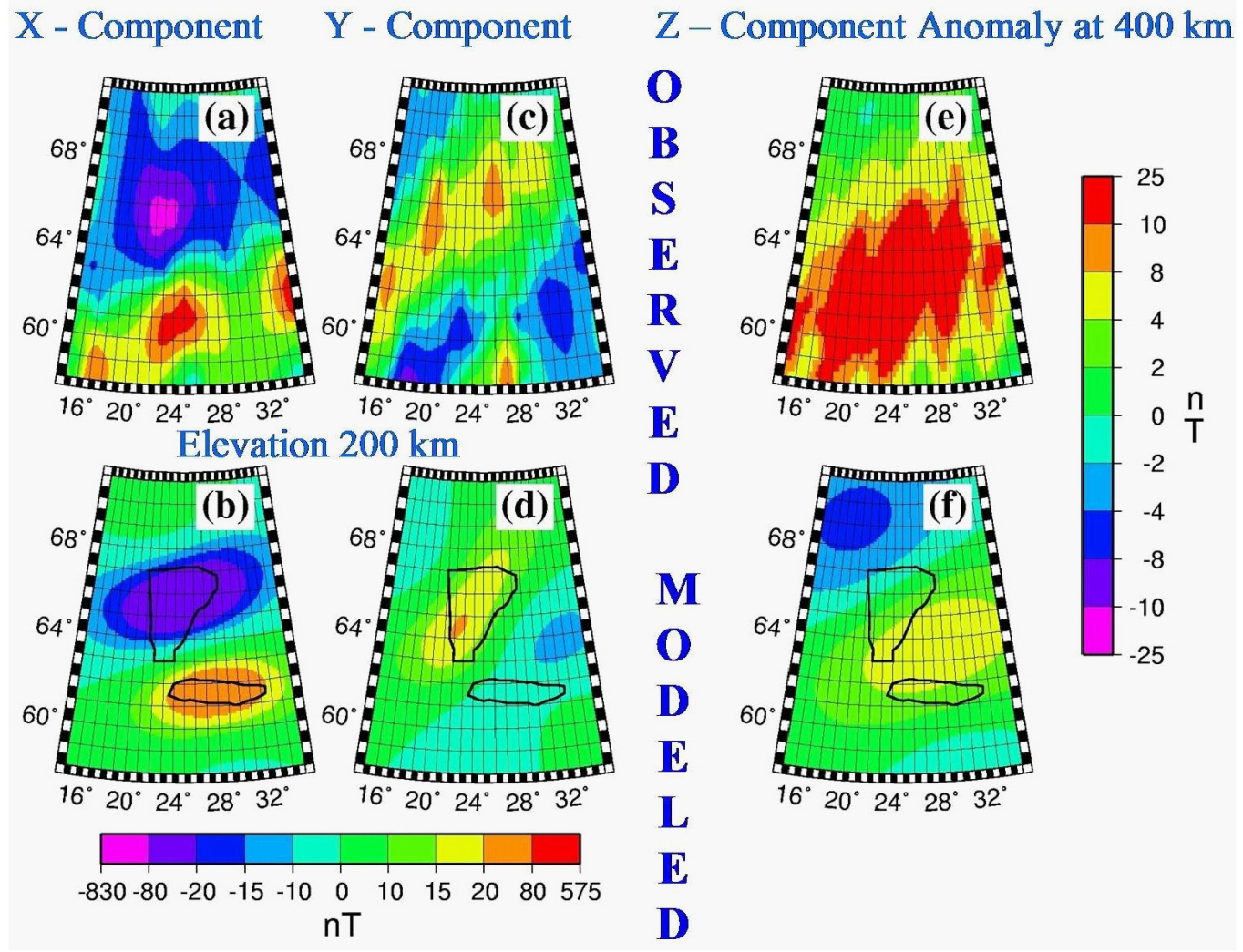


Figure 2.7. Observed and modeled fields of X, Y and Z (400 km) of anomaly – M3.

When the magnetization is near horizontal, the line joining the centers of the two lobes can be clearly identified and its angular distance with the azimuth could be defined as declination angle. Consequently, the direction of the paleopoles is well constrained. But when the magnetization is near vertical, there is only a single lobe and the declination and, consequently, the direction of paleopole is not well constrained. To illustrate the dispersion of paleopoles, the paleopoles computed from the modeled magnetization vectors (Table 1.2) are plotted in Figure 2.8. Magnetizations derived for M3 are more horizontal; this means that their declinations, which determine the direction of the paleopoles, are better constrained as a result of the dipolar pattern of the anomaly. However, for a horizontally magnetized source, the paleopole is far away from the source and therefore small declination differences in the magnetization directions of modeled sources will lead to significantly different paleopole locations. When many sources are analyzed, the errors will lead to large scatter in the pole locations. On the other hand, for anomalies that have predominantly a single lobe suggesting a near vertical magnetization direction for a single large source, the widely varying declination directions have very little influence in the scatter of the paleopoles. Even though the declination direction is not well-constrained, the distance to the paleopole is close enough and thus the scatter will essentially be within the range of the radius of the angular distance to the pole. Unfortunately, on Mars, there appear to be only few, about 14, isolated near horizontally magnetized anomalies (shown on Figure 1.1).

The dispersion in the paleopole locations is exacerbated if one considers alternative source models shown earlier (Figure 2.8). Even if one does not take into account the single source or segmented models of this study, the dispersion of paleopole locations of

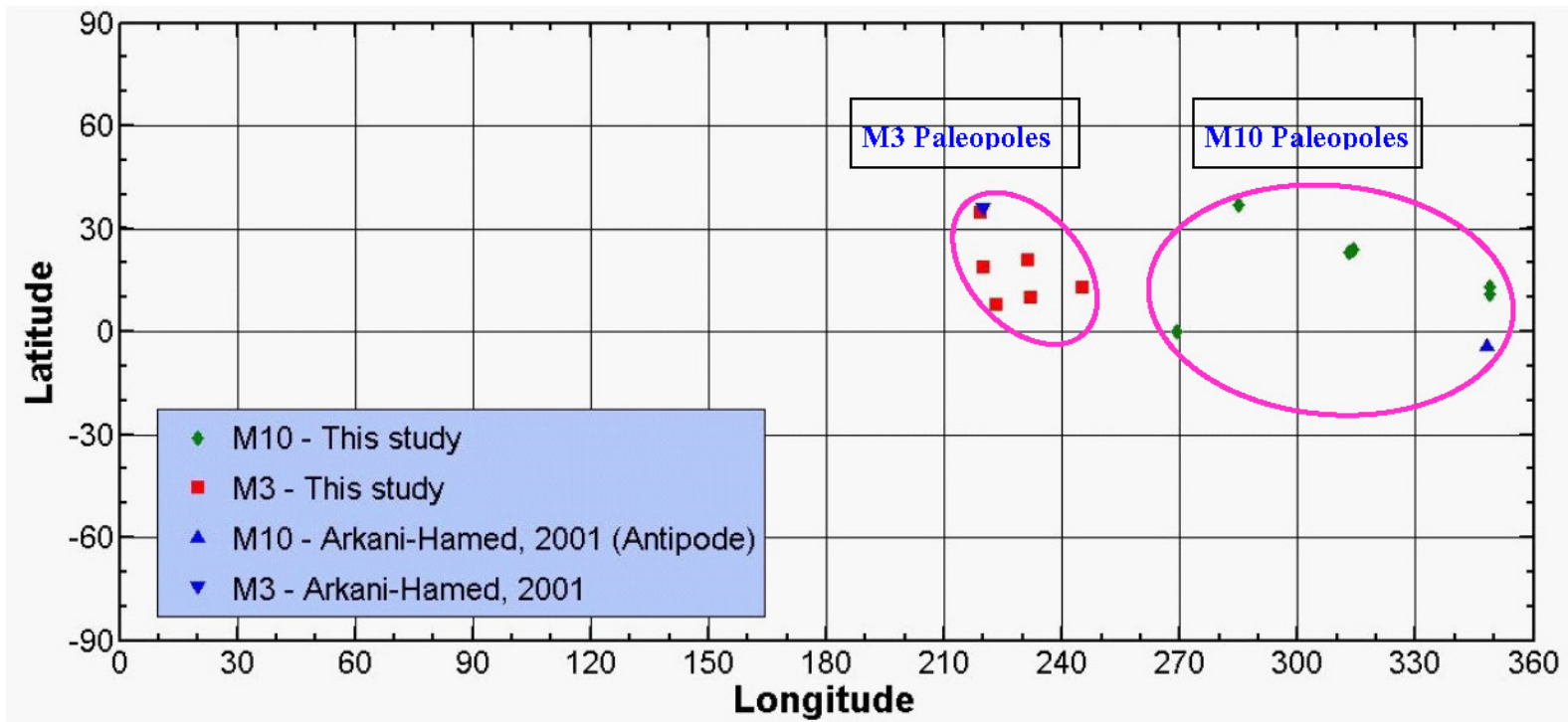


Figure 2.8. Scatter of paleopole locations from this study of anomalies M10 and M3 and from Arkani-Hamed, 2001. M10 (lat. 4°, long. 168°) and M3 (lat. 6°, long. 220°) (antipodes plotted for best clustering).

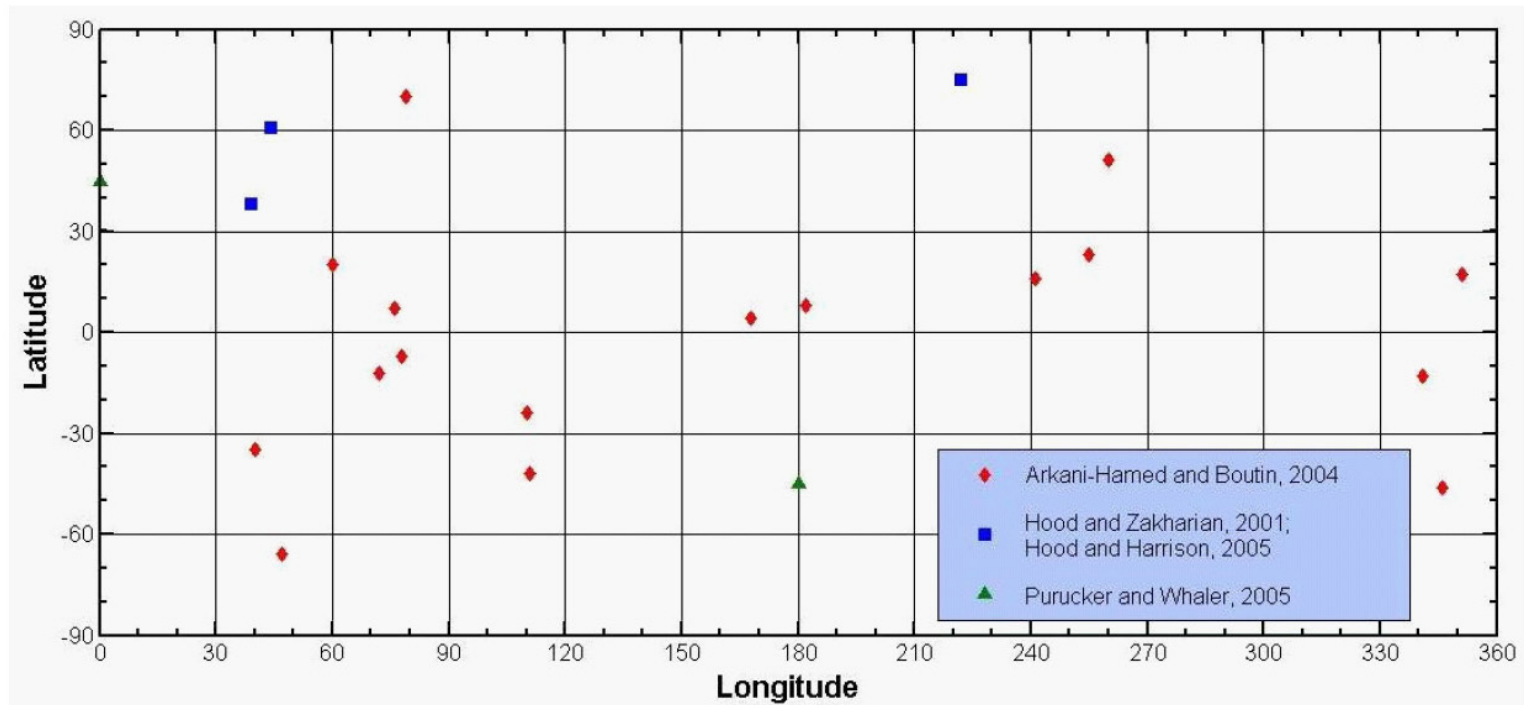


Figure 2.9. Scatter of paleopole locations computed by Arkani-Hamed and Boutin (2004), Hood and Zakharian (2001), Hood and Harrison (2005) and Purucker and Whaler (2005) – based on continuously varying magnetization model.

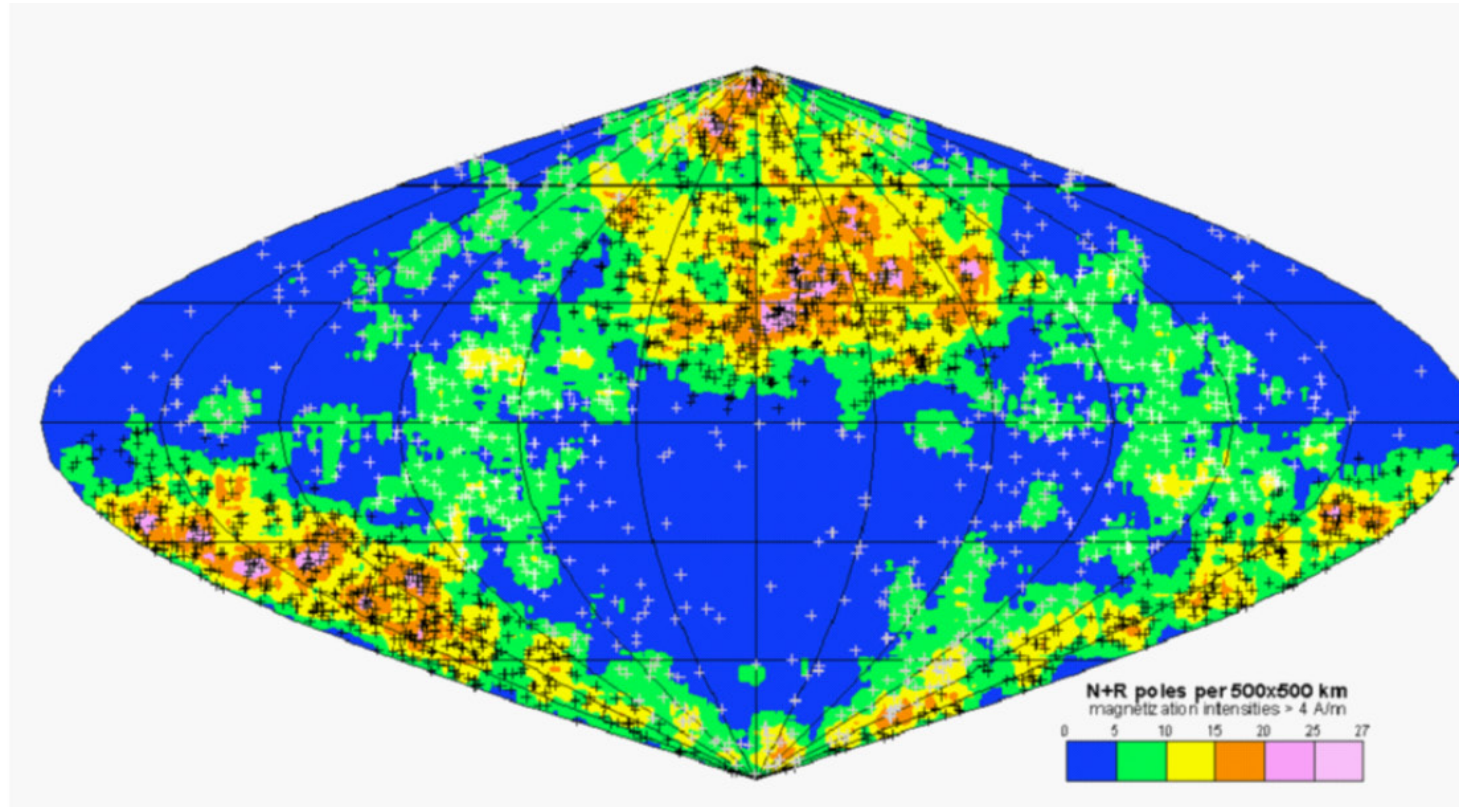


Figure 2.10. Figure from Phillips (2003) showing that when all sources with magnetization intensities of 4 A/m or higher are considered (as computed from Helbig method), the paleomagnetic pole positions are strongly concentrated within 50° of 195° E, 50° N as shown by the color contours and black symbols. A weaker concentration is seen with 40° of 290° E, 5° N (white symbols). The remaining solutions are scattered outside these concentrations (gray symbols).

all the previous workers is so large (Figure 2.9 and 2.10) that it is difficult to ascribe much significance to these pole locations. Furthermore, vastly different results are obtained by considering other modeling techniques and other anomalies. Based on modeling the southern highland linear magnetic anomalies (Figure 1.1), models of near-vertical magnetization by Connerney et al. (1999) and Ravat and Miller (2004) imply a pole near those anomalies. In addition, following different sets of logic, Hood and Harrison (2005) and Purucker and Whaler (2005) suggest pole location of 75°N , 222°E and 45°N , 0°E , respectively.

The effect of coalescence of magnetic anomalies at satellite altitude is explained in greater detail in the following section with the northeast America and neighboring Atlantic ocean magnetic anomalies from Earth, which are available at both near surface elevation and satellite altitudes.

CHAPTER 3

THE COALESCENCE EFFECT EXAMINED FROM NEAR SURFACE AND SATELLITE ALTITUDES

In this chapter, I will examine the magnetic anomaly maps of northeast America and neighboring Atlantic ocean region at near surface and satellite altitudes to show the coalescence effect. The near surface total intensity magnetic anomaly map of northeast America and neighboring Atlantic ocean (Figure 3.1) has patterns that reflect the subsurface geology and tectonics (e.g. the Appalachian sutures, the Grenville terranes, the seafloor spreading anomalies and the ocean quiet zones etc.). On the other hand, the total magnetic anomaly map of the same region at 150 km altitude, compiled by jointly inverting and continuing the near surface and Magsat data sets (based on the methods of Ravat et al., 2002) (Figure 3.2) is marked by large oval shaped highs and lows. It is observed that magnetic anomalies of many different geologic domains, formed at different times and having different magnetization directions on Earth, merge at high altitudes into collective features by virtue of the coalescence of anomalies. If modeled as single uniform magnetization, this coalescence in some cases will lead to false geologic interpretation and magnetization directions. Our purpose is to understand:

- Are our interpretations of anomalies at these two different elevations are similar? If true, this implies that modeling of the magnetic anomalies will likely lead to similar source characterization independent of whether the anomaly is observed at near surface elevation or satellite altitude.
- How well is the Amplitude of Analytic Signal (AAS) field able to guide the interpretation? Can the AAS field technique guide us towards more realistic

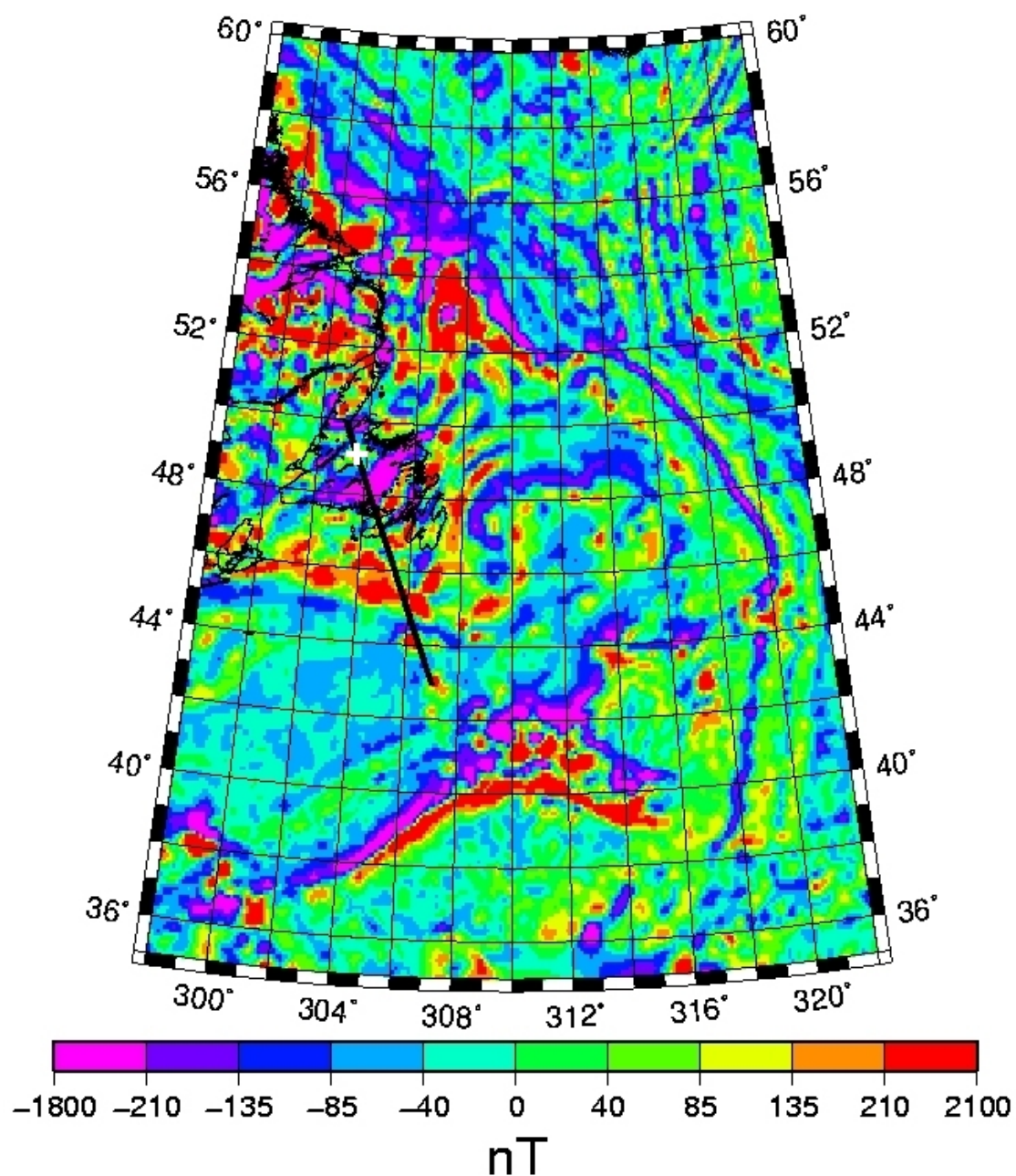


Figure 3.1. Total magnetic field anomaly map over northeast America and Atlantic ocean observed at the Earth's surface. The + symbol (303.5° E, 49° N) denotes the Dunnage volcanic complex having positive magnetic contrast with the surrounding rocks.

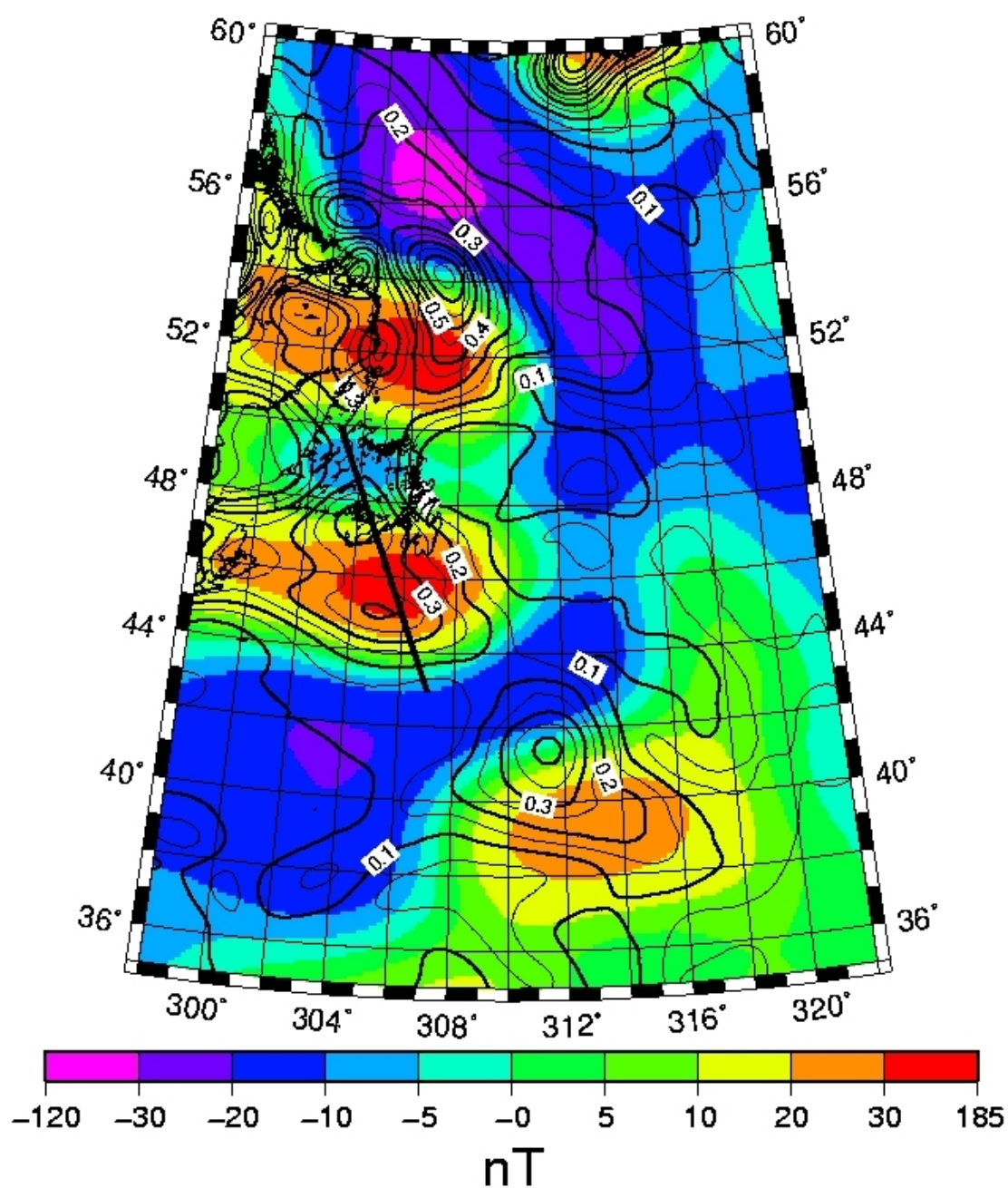


Figure 3.2. Total magnetic anomaly map over northeast America and Atlantic ocean observed at 150 km altitude. Smaller magnetic anomalies coalesce together forming large oval shapes of highs and lows. The contour lines represent the Analytic Signal field.

models of magnetic anomalies where we do not have adequate information of subsurface geology?

A part of the study area overlies the island province of Newfoundland. The island and the surrounding region have a very complicated geologic history with multiple phases of rifting and compression. Williams (1995) has documented the geology of this region in great detail. The island has four major geologic zones (Figure 3.3): the Humber, the Dunnage, the Gander and the Avalon. The Dunnage and Gander zones represent the Central Mobile Belt of the Appalachian foldbelt. The Humber zone is characterized by thrust sheets and nappes of mélanges and ophiolite sequences as a remanent feature of rifting within the ancient crust of North America followed by compression – the Taconic orogeny (450 Ma). The Dunnage zone is characterized by submarine volcanics and ophiolite sequences with overlying volcano clastic sediments. These rocks have positive magnetic anomaly signatures (e.g., Williams, 1995) compared to surrounding Humber and Gander zones. Metamorphosed pelitic and semi-pelitic rocks along with some igneous rocks characterize the Gander zone. They appear to be remanents of older deformation. The Gander zone would probably be reflected as magnetic low region in the near surface and 150 km elevation magnetic anomaly maps because of its predominant non-magnetic formations. The Avalon zone is different from the other zones. It is characterized by blocks of Precambrian volcanics and sedimentary deposits of Cambrian and Ordovician carbonates with some igneous magnetic rocks and clastic sediments overlying the Precambrian units. An unconformity separates the sedimentary and Precambrian sequences.

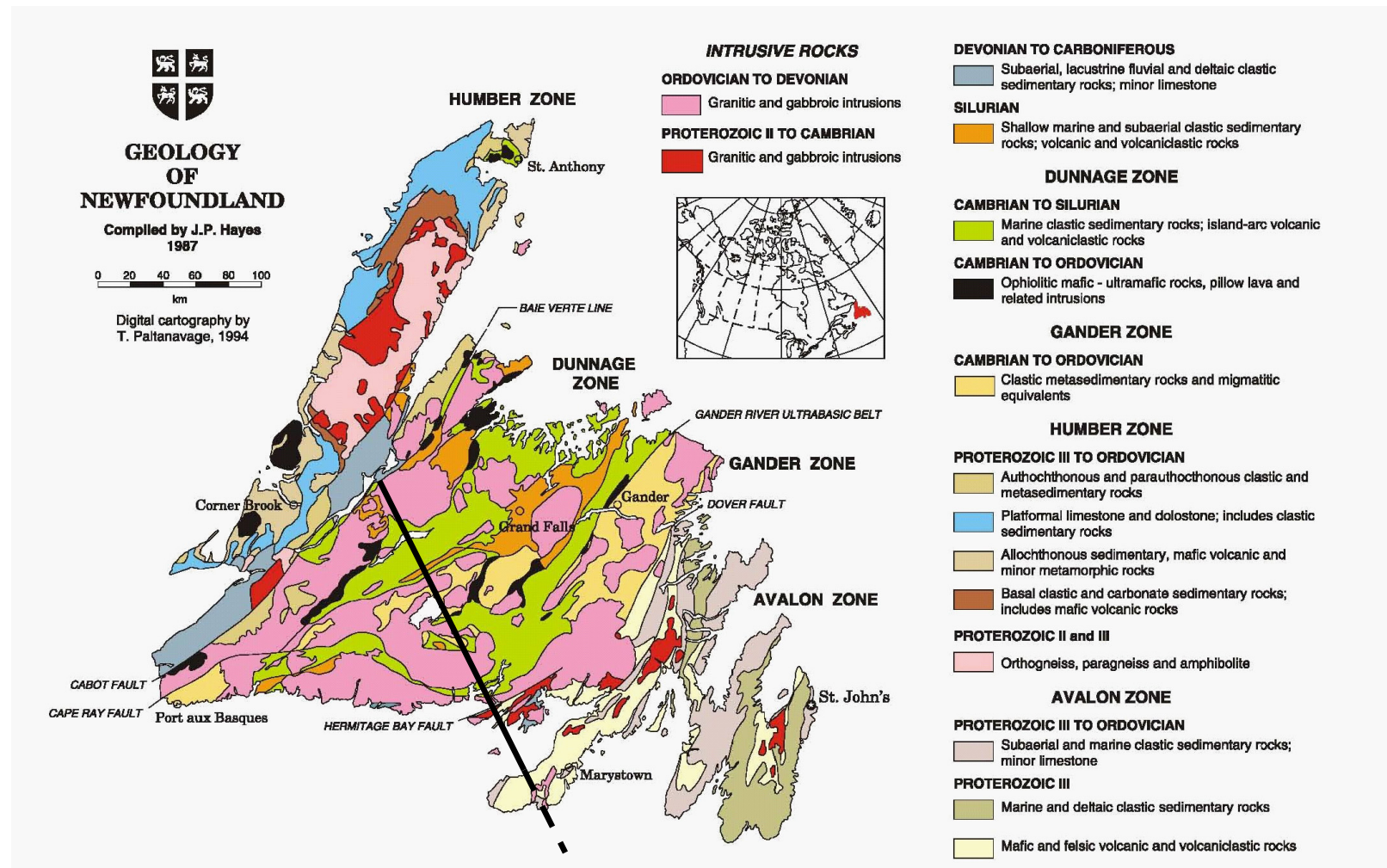


Figure 3.3. Map showing different geological zones of Newfoundland (from Hayes, 1987) and approximate profile location of the 2D magnetic anomaly model (figure 3.4).

In order to further investigate the problem of coalescence of magnetic anomalies at satellite altitude, I chose a NW-SE trending profile (C) across Dunnage, Gander and Avalon zones and the neighboring oceanic crust to model the anomaly both at near surface elevation and 150 km.

The 2D model (Figure 3.4) of the source for the anomaly at near surface elevation along the profile C shows a number of remanent and induced sources at shallow depths belonging to the Dunnage, the Gander and the Avalon zones and two large induced sources at depths close to 40 km: the Gander complex and the Avalon Precambrian complex respectively. The magnetic parameters of the different sources are listed in Table 3.1. It should be noted that the different lithologic sources near the transition of oceanic and continental crust, which are modeled as remanent sources have a large range of magnetization directions. This is reflected in the near surface anomaly as the short wavelength component. The first large and deeper induced source in the Avalon Precambrian complex has a positive susceptibility contrast with respect to the surrounding region. The second large and deeper induced source, the Gander complex, modeled as a wedge of low susceptibility material has a negative susceptibility contrast with the surrounding rocks (between 400 – 477 km on the horizontal axis on Figure 3.4). It is interesting to note that, as we have shown later in our multiple source model of the satellite altitude anomaly, these large induced sources might be reflected in the long wavelength of the satellite altitude anomaly. The intrusion at the far north end of the profile (between 470 – 490 km on Figure 3.4), a part of the Dunnage volcanics, is modeled as a remanent source with the magnetization vector defined by $I = 22^\circ$ and $D = 171^\circ$ (Johnson et al., 1991). Although, the modeled source is not shown exposed on the

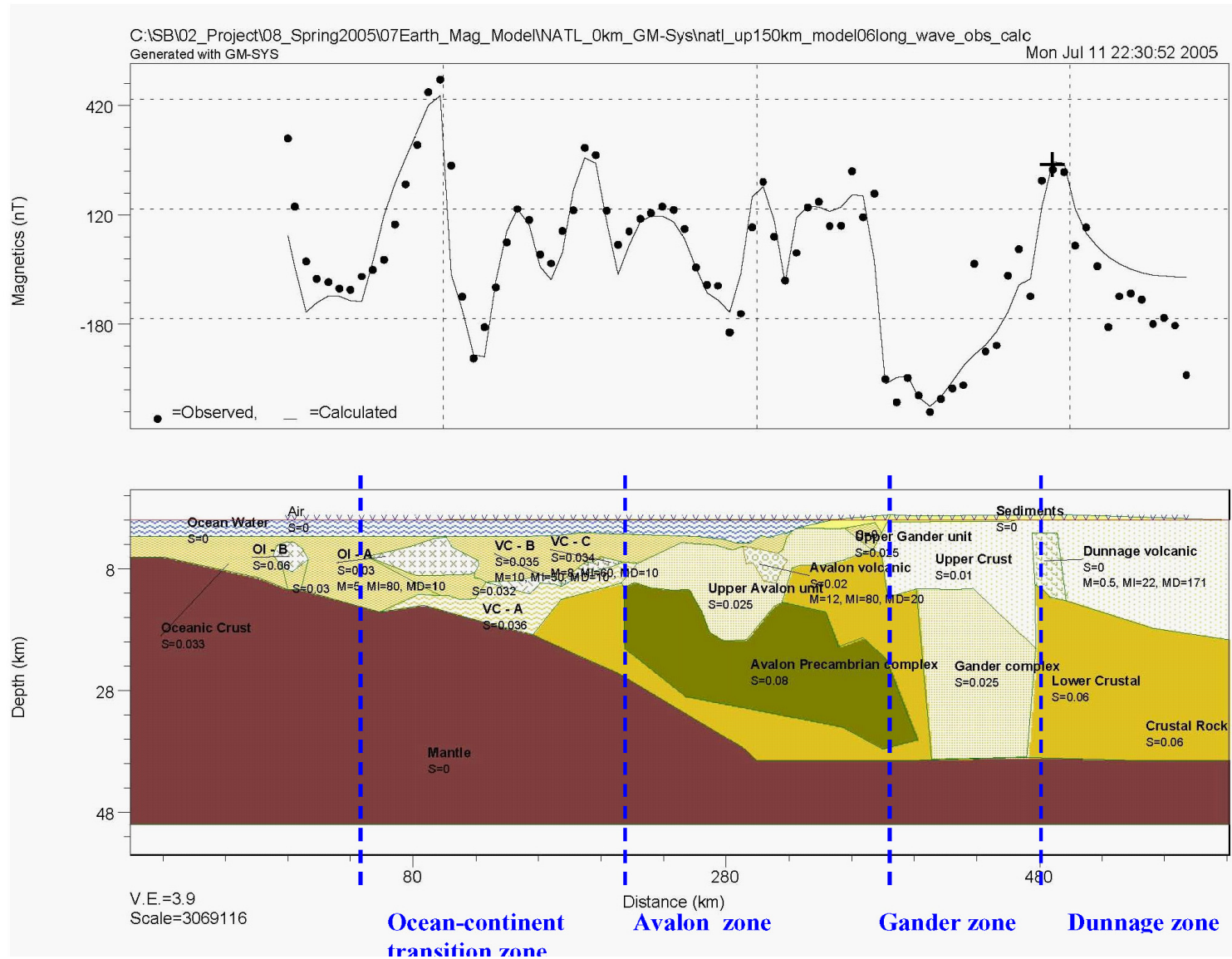


Figure 3.4. The 2D model of near surface elevation of magnetic anomaly along the profile. The + symbol denotes the Dunnage volcanic complex having positive magnetic contrast with surrounding rocks.

Table 3.1. Magnetic parameters of different sources of the 2D model (Figure 3.4) of the magnetic anomaly at near surface elevation.

Source	Modeled Magnetization (Strength, M , in A/m) or (Susceptibility, S , in SI units)	
Oceanic crust	Induced	$S = 0.033$
Oceanic intrusion A (OI-A)	Induced	$S = 0.060$
Oceanic intrusion B (OI-B)	Remanent	$I = 80^\circ, D = 10^\circ, M = 5$
Volcanic complex – A (VC-A)	Induced	$S = 0.036$
Volcanic complex – B (VC-B)	Remanent	$I = 50^\circ, D = 10^\circ, M = 10$
Volcanic complex – C (VC-C)	Remanent	$I = 60^\circ, D = 10^\circ, M = 8$
Upper Avalon unit	Induced	$S = 0.025$
Avalon Precambrian complex	Induced	$S = 0.080$
Avalon volcanic	Remanent	$I = 80^\circ, D = 20^\circ, M = 12$
Upper Gander unit	Induced	$S = 0.025$
Gander complex	Induced	$S = 0.025$
Upper Crust	Induced	$S = 0.010$
Dunnage volcanic	Remanent	$I = 22^\circ, D = 171^\circ, M = 0.5$ (Johnson et al. ,1991)
Lower Crust	Induced	$S = 0.060$

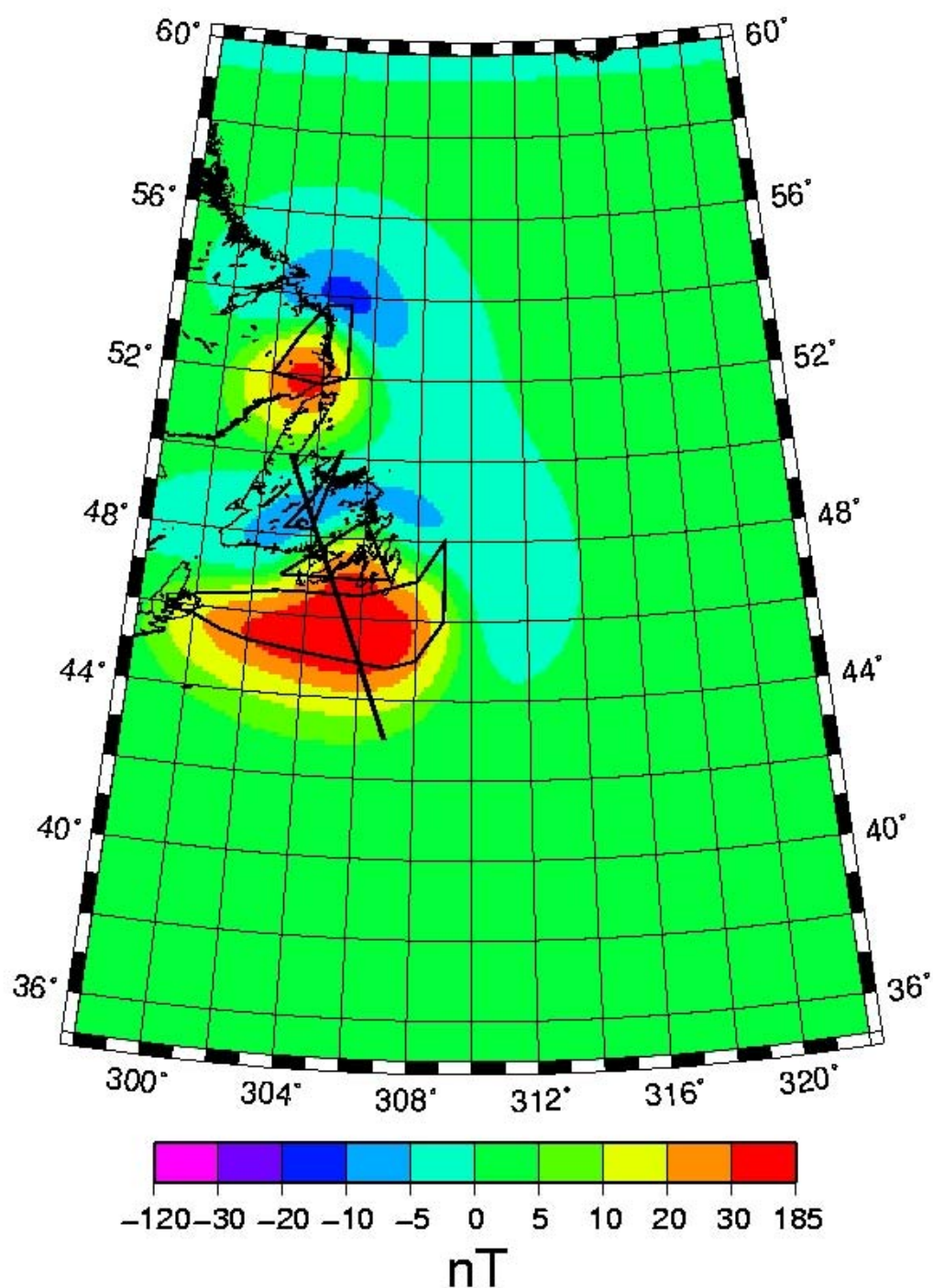


Figure 3.5. The 3D model of the satellite altitude magnetic anomaly with multiple sources following Amplitude of Analytic Signal contours and geology as the guideline.

surface, Pariso and Johnson (1993) have suggested, based on magnetic petrology from ocean drill core data, that lower oceanic crustal rocks can have strong remanent magnetization.

The 3D multiple source model (Figure 3.5) (using Program SPHEREII by von Frese et al. (1981) and Ravat. (1989)) of the anomaly at satellite altitude is derived using the previously outlined procedure with the AAS field as a guide to model the sources, modified as indicated by the geology of the region reflected in the near surface magnetic anomaly map. The model shows two induced and two remanent sources as outlined by the polygons. The first polygon in the south, the ocean-continent transition zone complex, is a large induced source with positive susceptibility contrast with the surrounding rocks. It is located between depths of 3 and 40 km. The second polygon – the Avalon complex is a remanent source (see Table 3.2 for magnetic parameters and modeled depth extent). The third polygon – the Gander complex is a wedge shaped induced source with negative susceptibility contrast with the surrounding rocks. The fourth and final polygon – the Humber complex zone is another remanent source. The two deeper and induced sources used in 3D model of the satellite altitude anomaly are modeled similarly in the 2D model of the anomaly (Figure 3.4). The fit of our 3D model and the observed anomaly along the profile is shown in Figure 3.6. An alternative model, based only on the 150 km altitude magnetic anomaly features, is the single, nearly elliptical source model of the satellite altitude anomaly as shown in Figure 3.7. This source has both induced and remanent magnetization components (Table 3.2). The disadvantage of a single source model is that in addition to being over simplified in nature, it does not incorporate the geological

Table 3.2. Magnetic parameters of different sources of the 3D models (Figures 3.5 and 3.7) of the magnetic anomaly at altitude of 150 km.

Source		Depth (km)	Modeled Magnetization (Strength, M , in A/m) or (Susceptibility, S , in SI units)	
Multiple sources	Ocean-continent transition complex	3 – 40	Induced	$S = 0.0018$
	Avalon complex	0 – 20	Remanent	$I = 60^\circ$, $D = 330^\circ$, $M = 2.5$ A/m
	Gander complex	0 – 40	Induced	$S = -0.0002$
	Humber complex	0 – 20	Remanent	$I = 30^\circ$, $D = 20^\circ$, $M = 3.0$ A/m
Single source		0 – 40	Induced, $S = 0.003$	
			Remanent, $I = -45^\circ$, $D = 320^\circ$, $M = 1.5$ A/m	

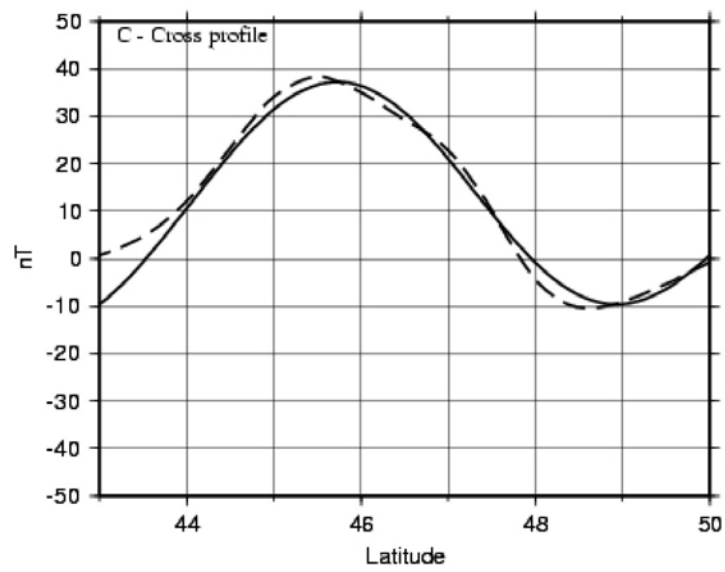


Figure 3.6. Fit of observed (continuous) and computed (dashed) Z-component fields for the model in Figure 3.5 along the profile.

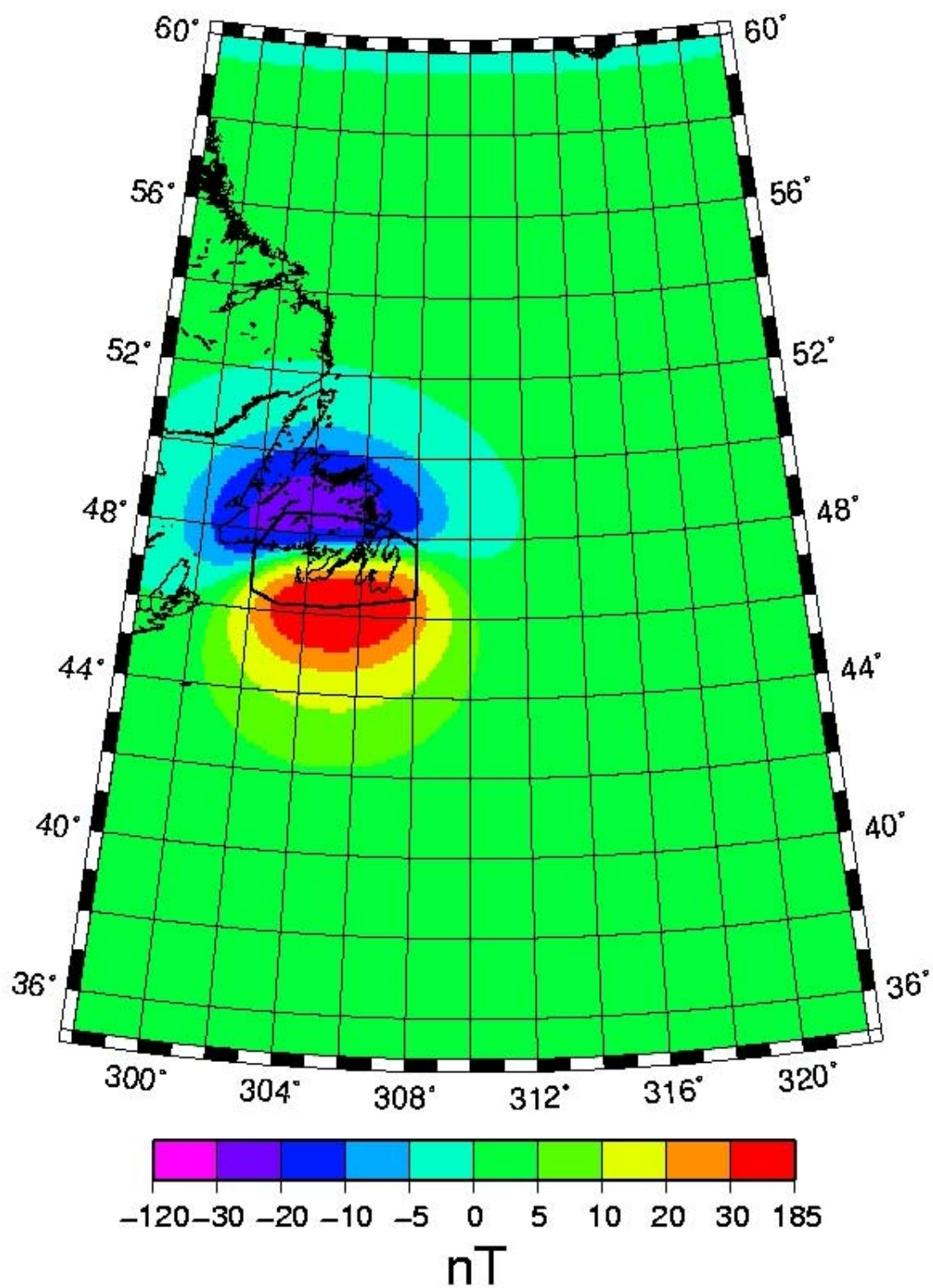


Figure 3.7. The 3D model of the satellite altitude magnetic anomaly with a single source.

information of the region, which is an important criterion for a model to realistically represent the observed magnetic anomaly.

Based on the above models at near surface and satellite altitudes, it is evident that much of the short wavelength component of the magnetic anomaly at near surface elevation is related to the sources at shallow depths and this is not reflected in the magnetic anomaly at satellite altitude. The exception is the zone of low susceptibility that goes through the whole crust in the Gander zone between 400 – 477 km on the horizontal axis. Much of the anomaly at satellite altitude is controlled by sources at depths below 20 km. Although, I suggest that the sources for the magnetic anomalies at these two different altitudes are different in their depth location it is possible that a few large sources might have a bearing on the magnetic anomalies at both near surface and satellite altitudes, for example, the Gander complex source appears both in the near surface and satellite altitude anomaly. This example suggests that most of the deep seated sources reflected in the satellite and near surface data can have similar attributes. But as indicated by the alternative single source model created to represent the dipolar anomaly at 47°E and 305°W (Figure 3.7), it is not possible to say that modeling of satellite altitude magnetic anomaly will always lead to meaningful and realistic source characterizations. It is also evident comparing the Figure 3.2 (observed anomaly at 150 km), Figure 3.5 (multiple source model) and Figure 3.7 (single source model) that multiple source models of magnetic anomalies at satellite altitudes are better suited for representing a realistic geological scenario compared to single circular or elliptical prismatic sources. Most of the sources modeled at shallow depths following the near surface elevation magnetic anomaly are masked at satellite altitudes by virtue of anomaly attenuation. Thus, in spite

of the suggestion that multiple source bodies might be better suited to represent realistic geological scenarios for modeling magnetic anomalies at satellite altitude, in the absence of complementary information from the geology of the region, the interpretation is limited by the coalescence effect. However, based on the final modeled sources derived from AAS field and the geology (Figures 3.5), it can be concluded that the AAS field technique can guide us towards at least a few of the geologically meaningful sources even if it cannot capture all aspects of geology (as shown by the examples on the Earth).

CHAPTER 4

DISCUSSION

Isolated magnetic anomalies observed by the Mars Global Surveyor spacecraft have been commonly interpreted as caused by large elliptical or circular sources (Arkani-Hamed, 2001, 2002, 2003, 2004; Hood and Zakharian, 2001; Richmond and Hood, 2003). In this study, the segmented multiple source model for anomaly M10 and anomaly M3 have illustrated that multi-source models are valid for magnetic anomalies on Mars because of the ambiguity in source configurations of potential fields (e.g. Green's theorem of equivalent layer in Blakely, 1995). Single source circular or elliptical geometry models are less realistic when compared to geologic magnetization variations seen on the Earth. A few of the segments in these multiple source models of M10 and M3 are magnetized in completely different directions compared to the models of previous workers (see Table 1.2 for details). This variation in magnetization of the different segments of the multiple source models is not evident in the magnetic field observations at satellite altitudes around 150 km or higher because of the coalescence effect. However, mapping the magnetic anomaly of segmented model of M10 at lower altitudes (Figure 2.4) clearly reveals the different zones of magnetization. It is thus implied that magnetic anomaly observation at satellite altitude could be easily misinterpreted, especially, in absence of the detailed geological or geophysical knowledge of the region. Taylor and Ravat (1995) have also previously suggested that the coalescence effect poses a serious challenge in the interpretation of magnetic anomalies at satellite altitudes.

The paleopoles computed from the models M10 and M3 made of many small blocks cover roughly 40% of the surface of Mars. However, the large source models and the paleopoles derived from them could be meaningful under the following conditions:

- Small lateral lithospheric movement between the sources of identified anomaly since acquisition of their magnetization. This ensures that all the different sources would appear magnetically coherent when observed from higher altitudes, leading to similar magnetization vectors interpreted from the different sources.
- Correct estimation of the source geometry, shape and size, otherwise the model would lose its geologic relevance. In addition, different shaped sources producing similar anomalies could be interpreted as having different magnetization vectors leading to increased scattering in paleopoles.

Unless these special circumstances are called for, paleopoles derived from these sources could have problems. More recently, Arkani-Hamed and Boutin (2004) have also recognized that even small changes in source geometry such as elliptical vs. circular prisms, can lead to difference in derived magnetization directions as large as 15° .

Based on the models of magnetic anomalies over northeastern America and neighboring Atlantic Ocean derived in this study to learn from earth-based comparisons, geologically realistic sources can vary from a few meters to 100s of km in dimensions. The 2D model (Figure 3.4) of the magnetic anomaly at near surface elevation shows that the sources of short-wavelength anomalies are present at shallow depths (less than 20 km). The effect of these shallow sources attenuates with increasing observation elevation. However, the effect of a large deeper source in the Gander complex is evident in both the anomalies at near surface and satellite altitudes. It is modeled as a relatively low susceptibility source in both the near surface (2D) and satellite altitude (3D) models (Figure 3.5). The 3D model of the anomaly at satellite altitude is derived using the AAS

field, subsequently modified by the geology of the region. This implies that interpretation of satellite altitude magnetic anomaly, aided by AAS field and knowledge of the geology of the region, may lead to geologically realistic source configurations.

Most researchers have been puzzled with large apparent magnetization on Mars (Kletetschka et al., 2000a; Kletetschka et al., 2000b; Hargraves et al., 2001; Scott and Fuller, 2004; Kletetschka et al., 2005); however, the situation is likely to be even more drastic. I have calculated the magnetization contrast multiplied by volume for my large single source models and the segmented models for both M10 and M3 anomalies. The value for the single source M10 model is 11016 Akm^2 and multiple source segmented model (Figure 2.2) is 35100 Akm^2 . The corresponding values for the M3 models are 28080 Akm^2 and 42480 Akm^2 (Figure 2.5), respectively. For both the anomalies, the value for the segmented model is 2-3 times higher than the single source model. This is explained by the coalescence effect. Because of coalescence, the short-wavelength variation in magnetization is attenuated and not evident in the large, single source model inferred from high altitude. It is thus probable, that the real magnetization contrasts on Mars are much higher than what is apparent with single sources.

CHAPTER 5

CONCLUSION

The magnetic source models generated in this study based on the anomalies designated as M10 and M3 on Mars show that, in addition to the current large elliptical or circular source models (Arkani-Hamed, 2001, 2002, 2003, 2004; Hood and Zakharian, 2001), the anomalies could be produced by coalescence of anomalies from small sources having a number of different sets of magnetization directions. The paleopoles computed from the resulting magnetization vectors based on the dipolar main field hypothesis are spread over a large part of the planet.

The models of magnetic anomalies observed on Earth over northeast America and neighboring Atlantic ocean at near surface and 150 km elevation show that a model consisting of small, multiple sources at shallow depths and large sources at greater depths could be geologically realistic. It would be reasonable to believe that this situation might be applicable to the situation on Mars. Since we do not have magnetic field observation at low altitudes on Mars, the data from satellite altitude would reflect only deep-seated sources rather than shallow geologic magnetic variations that are commonly used to infer paleopoles. At high altitudes, much of the information attributed to the local variations in the anomalies would be lost due to anomaly attenuation.

Understanding the tectonic significance of the magnetic anomaly patterns on Mars requires low altitude magnetic anomaly measurements in future. Such a mission would be able to resolve the source structure of the crustal magnetism of the planet. An airplane flying at elevations of a few kilometers with a magnetometer on board could be used for such a low altitude mission covering at least a small portion of the planet, and could

reveal regional tectonic patterns as observed on Earth by aeromagnetic surveys. A rover, similar to Opportunity and Spirit on Mars, fitted with a magnetometer could also be used for conducting very high resolution magnetic anomaly surveys on Mars in an attempt to examine the importance of extreme near-surface magnetic variation.

REFERENCES

- Acuña, M.H., Connerney, J.E.P., Ness, N.F., Lin, R.P., Mitchell, D., Carlson, C.W., McFadden, J., Anderson, K.A., Rème, H., Mazelle, C., Vignes, D., Wasilewski, P., and Cloutier, P., 1999, Global Distribution of Crustal Magnetization Discovered by the Mars Global Surveyor MAG/ER Experiment: *Science*, v. 284, p. 790-793.
- Acuña, M. H., Connerney, J.E.P., Wasilewski, P., Lin, R.P., Mitchell, D., Anderson, K.A., Carlson, C.W., McFadden, J., Rème, H., Mazelle, C., Vignes, D., Bauer, S.J., Cloutier, P., and Ness, N.F., Magnetic field of Mars: Summary of results from the aerobraking and mapping orbits: *Journal of Geophysical Research*, v.106, no. E10, p. 23403-23417.
- Arkani-Hamed, J., 2001, Paleomagnetic Pole Positions and Pole Reversals of Mars: *Geophysical Research Letters*, v.28, no. 17, p. 3409-3412.
- Arkani-Hamed, J., 2002, Magnetization of the Martian crust: *Journal of Geophysical Research*, v.107, no. E5, p. 8-1 to 8-10.
- Arkani-Hamed, J., and Boutin, D., 2003, Polar Wander of Mars: Evidence from Magnetic Anomalies: Sixth International Conference on Mars, Abstract 3051.
- Arkani-Hamed, J., and Boutin, D., 2004, Paleomagnetic poles of Mars: Revisited: *Journal of Geophysical Research*, v.109, no. E03011.
- Biswas, S., and Ravat, D., 2005, Why meaningful paleopoles can't be determined without special assumptions from Mars Global Surveyor data?: Lunar and Planetary Science Conference, XXXVI, abstract 2192.
- Blakely, R.J., *Potential theory in gravity and magnetic applications*, 437 pp., Cambridge Univ. Press., 1995.
- Butler, R.F., *Paleomagnetism: Magnetic domains to geologic terranes*, 319 pp., Blackwell Sci., Malden, Mass., 1992.
- Carporzen, L., Gilder, S.A., and Hart, R.J., 2005, Paleomagnetism of the Vredefort meteorite crater and implications for craters on Mars: *Nature*, v. 435, p. 198-201.

- Connerney, J.E.P., Acuña, M. H., Wasilewski, P.J., Ness, N.F., Rème, H., Mazelle, C., Vignes, D., Lin, R.P., Mitchell, D.L., and Cloutier, P.A., 1999, Magnetic Lineations in the Ancient Crust of Mars: *Science*, v. 284, p. 794-798.
- Connerney, J.E.P., Acuña, M. H., Wasilewski, P.J., Kletetschka, G., Ness, N.F., Rème, H., Lin, R.P., and Mitchell, D.L., 2001, The Global Magnetic Field of Mars and Implications for Crustal Evolution: *Geophysical Research Letters*, v. 28, no. 21, p.4015-4018.
- Dunlop, D.J., 2005, Magnetic impact craters: *Nature*, v. 435, p. 156-157.
- Frawley, J.J., and Taylor, P.T., 2004, Paleo-pole positions from martian magnetic anomaly data: *Icarus*, v. 172, p. 316-327.
- Hargraves, R.B., Knudsen, J.M., Madsen, M.B., and Bertelsen, P., 2001, Finding the right rocks on Mars: *Eos Transactions AGU*, v. 82, no. 26, p. 292.
- Hayes, J.P., 1987, *Geology of Newfoundland*.
- Hood, L.L., and Zakharian, A., 2001, Mapping and modeling of magnetic anomalies in the northern polar region of Mars: *Journal of Geophysical Research*, v. 106, no. E7, p. 14601-14619.
- Hood, L.L., and Harrison, K.P., 2005, Are Martian crustal magnetic anomalies and valley networks concentrated at low paleolatitudes?: *Lunar and Planetary Science Conference*, XXXVI, abstract 1110.
- Johnson, Rex J.E., van der Pluijm, Ben A., Van der Voo, Rob, 1991, Paleomagnetism of the Moreton's Harbour Group, Northeastern Newfoundland Appalachians: Evidence for an Early Ordovician island arc near the Laurentian margin of Iapetus: *Journal of Geophysical Research*, v. 96, no. B7, p. 11689-11701.
- Kletetschka, G., Wasilewski, P.J., and Taylor, P.T., 2000a, Hematite vs. magnetite as the signature for planetary magnetic anomalies?: *Physics of the Earth and Planetary Interiors*, v. 119, p. 259-267.

- Kletetschka, G., Wasilewski, P.J., and Taylor, P.T., 2000b, Mineralogy of the sources for magnetic anomalies on Mars: *Meteoritics and Planetary Science*, v. 35, p. 895-899.
- Kletetschka, G., Ness, N.F., Connerney, J.E.P., Acuna, M.H., and Wasilewski, P.J., 2005, Grain size dependent potential for self generation of magnetic anomalies on Mars via thermoremanent magnetic acquisition and magnetic interaction of hematite and magnetite: *Physics of Earth and Planetary Interiors*, v. 148, p. 149-156.
- Langlais, B., Purucker, M.E., Manda, M., 2004, Crustal magnetic field of Mars: *Journal of Geophysical Research*, v. 109, no. E02008.
- Lillis, R.J., Manga, M., Mitchell, D.L., Lin, R.P., and Acuña, M. H., 2005, Evidence for a second Martian dynamo from electron reflection magnetometry: *Lunar and Planetary Science Conference*, XXXVI, abstract 1578.
- Pariso, J.E., and Johnson, H.P., 1993, Do lower crustal rocks record reversals of the Earth's magnetic field? Magnetic petrology of oceanic gabbros from Ocean Drilling Program Hole 735B: *Journal of Geophysical Research*, v. 98, no. B9, p. 16013-16032.
- Phillips, J. D., 2003, Martian magnetization vectors estimated from Helbig analysis supports a reversing core dynamo: *Eos Transactions AGU*, v. 84, no. 46, Fall Meeting Supplement, abstract GP21A-0031.
- Purucker, M.E., Ravat, D., Frey, H., Voorhies, C., Sabaka, T., and Acuña, M. H., 2000, An altitude-normalized magnetic map of Mars and its interpretation: *Geophysical Research Letters*, v. 27, p. 507-510.
- Purucker, M.E., and Whaler, K.A., 2005, A Martian paleomagnetic pole estimate made using the distribution and intensity of large scale magnetic features: *Lunar and Planetary Science Conference*, XXXVI, abstract 1720.
- Ravat, D., 1989, Magsat investigations over the greater African region, Ph.D. Dissertation, Purdue University, West Lafayette, IN, 234p.
- Ravat, D., Whaler, K.A., Pilkington, M., Sabaka, T., and Purucker, M., 2002: Compatibility of high-altitude aeromagnetic and satellite-altitude magnetic anomalies over Canada. *Geophysics*. v. 67, p. 546-554.

- Ravat, D., and Miller, J., 2004, Analytic Signal in the interpretation of Mars southern highlands magnetic field: Lunar and Planetary Science Conference, XXXV, abstract 1047.
- Richmond, N.C., and Hood, L.L., 2003, Paleomagnetic pole positions of Mars: Lunar and Planetary Science Conference, XXXIII, abstract 1721.
- Schubert, G., Russell, C.T., and Moore, W.B., 2000, Timing of the Martian dynamo: *Nature*, v. 408, p. 666-667.
- Scott, E.R.D., and Fuller, M., 2004, A possible source for the Martian crustal magnetic field: *Earth and Planetary Science Letters*, v. 220, p. 83-90.
- Taylor, P.T., and Ravat, D., 1995, An interpretation of the Magsat anomalies of central Europe: *Journal of Applied Geophysics*, v. 34, p. 84-91.
- Von Frese, R.R.B., Hinze, W.J., Braile, L.W., and Luca, A.J., 1981, Spherical-Earth gravity and magnetic anomaly modeling by Gauss-Legendre Quadrature Integration: *Journal of Geophysics*, v. 49, 234-242.
- Williams, H., 1995, Geology of the Appalachian-Caledonian orogen in Canada and Greenland. Geological Survey of Canada, Geology of Canada, No. 6.

VITA

Graduate School
Southern Illinois University

Saurav Biswas
514, South Wall Street, Carbondale, IL 62901

Date of Birth: October 14, 1978

Calcutta University, Presidency College, India
Bachelor of Science, Geology, June 2000

University of Pune, India
Master of Science, Space Sciences, May 2002

Special Honors and Awards:

Awarded 'excellent' in the certificate given by PRL and Indian Space Research Organisation (ISRO) in a workshop on '**Meteorites, Asteroids, and Planets**' held in PRL in February – 2001

Thesis Title:

Non-uniqueness of the modeled magnetization vectors used in determining paleopoles on Mars

Major Professor: Dr. Dhananjay Ravat

Publications:

Biswas S., Ravat D. (2005) Why meaningful paleopoles can't be determined without special assumptions from Mars Global Surveyor data? 36th Lunar and Planetary Science Conference, Abstract 2192.

McBride, John H., Bexfield, Christopher E., Pugin, Dr. Andre, Ravat, Dhananjay, and **Biswas, Saurav**, (2005), Integration of high-resolution seismic reflection and micro-gravity techniques to improve interpretation of shallow subsurface structure: New Madrid seismic zone. GSA Rocky Mountain Section – 57th Annual Meeting, Abstract 87042.